Inhibition of Kynurenine aminotransferase

Dijkman, Ulrike

Chapter 4

Synthesis and biological evaluation of kynurenine derivatives as KAT inhibitors: Quinolinones

4.1 Introduction

Kynurenine (KYN, **4.1**) is the key intermediate in the kynurenine pathway, the major pathway of tryptophan metabolism. KYN is metabolized by kynureninase (KYNase), kynurenine 3-hydroxylase (kynurenine mono-oxygenase, KMO) and kynurenine aminotransferase (KAT). KAT catalyzes the reaction of KYN into kynurenic acid (KYNA). KYNA is an antagonist at the strychnine insensitive glycine coagonist site of NMDA receptors and a non-competitive antagonist at α7* nicotinic acetylcholine receptors. At much higher concentrations, KYNA is an antagonist at all ionotropic glutamate receptors and an agonist at orphan GPR35 receptors.[1-5] KYN metabolism by KYNase and KMO results in the formation of 3-hydroxykynurenine (3-OH-KYN), anthranilic acid (AA) and quinolinic acid (QUIN). QUIN is a precursor of NAD^+ and has neurotoxic properties.
Imbalances of the kynurenine pathway are associated with several disorders of the central nervous sytem. Upregulation of tryptophan metabolism into the kynurenine pathway leads to formation of neurotoxic 3-OH-KYN and QUIN. Elevated levels of 3-OH-KYN and QUIN are associated with Huntington's disease.[6-8] Elevated levels of KYNA have been found in patients suffering from schizophrenia.[9-11] KYNA is thought to impair cognitive function.[12]

This study aims for the design of compounds that pharmacologically decrease KYNA levels in the brain. For this purpose, inhibitors are desired that are selective towards KAT over KYNase and KMO. Conformationally restricted KYN analogs **4.2** and **4.3** were designed (Scheme 1).

Scheme 1

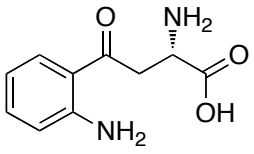

4.1

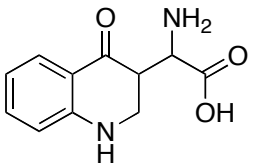

4.2

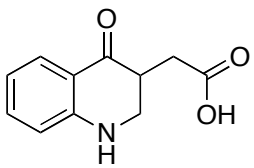

4.3

In these structures, the conformation of KYN is restricted by introduction of a methylene bridge between the aromatic amino group and the β-CH_2 group. In analog **4.3**, the α-amino-group is omitted. The compounds were synthesized and their ability to inhibit rat brain KAT and rat liver KYNase and KMO was tested.

4.2 Chemistry

4.2.1 Synthesis of 2,3-dihydro-4(1*H*)-quinolinone

2,3-Dihydro-4(1*H*)-quinolinone (**4.4**) is the core structure for the compounds of this study. The structure is known from literature. The substance is colored brightly yellow. The color is caused by extensive possibilities of tautomerism into tautomers B, C, D and E (Scheme 2).[13-15]

Scheme 2

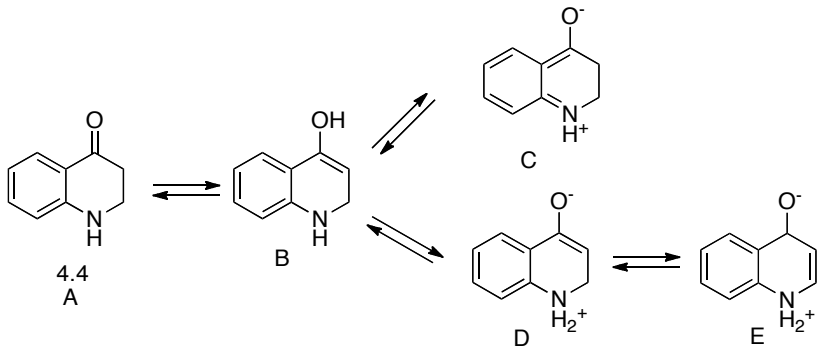

In order to stabilize intermediates and prevent aromatization or other ways of decomposition, proper protection of functional groups is essential in synthetic procedures.

Synthesis of the core structure was accomplished by published methods, according to Scheme 3.[13-15]

Scheme 3

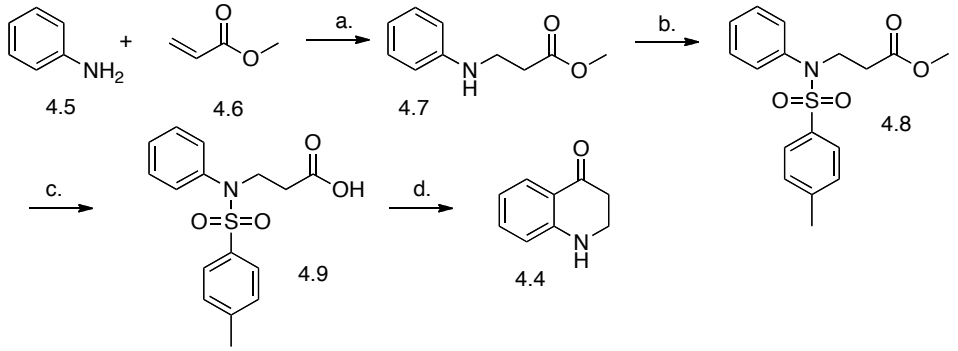

Reagents and conditions: a. acetic acid, 80°C; b. p-TosCl, pyridine, 25 min, r.t., then reflux 1 h; c. KOH/H_2O, MeOH; d. PPA.

Briefly, addition of aniline to methylacrylate in the presence of acetic acid yielded methyl ester **4.7**. The amine was then protected with para-toluene sulfonyl chloride (p-TosCl). The ester of tosyl-protected product **4.8** was hydrolyzed. Product **4.9** was subjected to ring-closure with PPA to obtain the brightly yellow colored product **4.4**.

4.2.2 Synthesis of amino-(4-oxo-1,2,3,4-tetrahydroquinolin-3-yl)-acetic acid

From core structure **4.4** different synthetic strategies were applied in order to finally obtain product **4.2**. In the first attempt, the tosyl-protected quinolinone **4.10** was brominated at the 3-position, followed by attempted coupling with diethylacetamidomalonate (Scheme 4).

Scheme 4

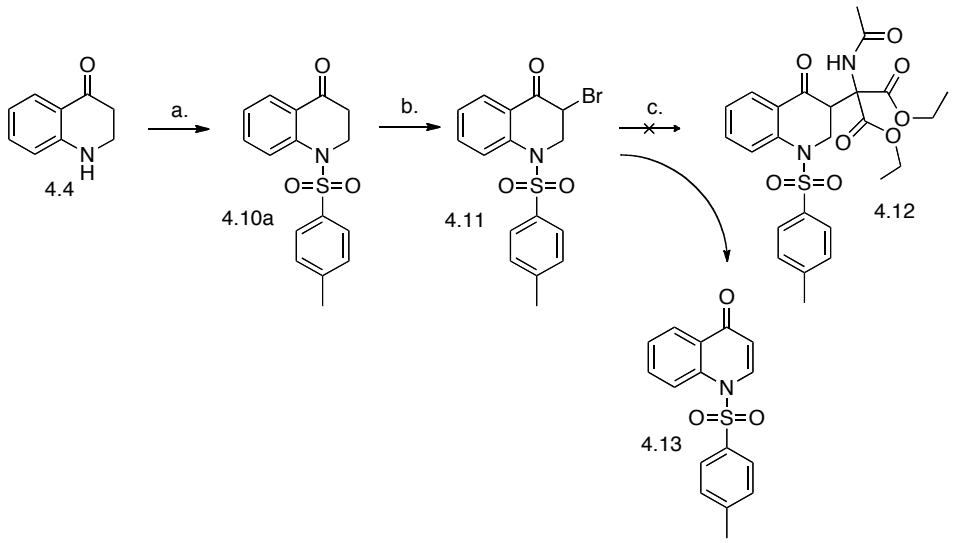

Reagents and conditions: a. p-TosCl, pyridine, 25 min, r.t., then 1.25h, 95 °C; b. Br_2, CH_3Cl; c. NaH, diethylacetamidomalonate, DMF.

This strategy had been employed successfully before in many monocyclic and some bicyclic KYN derivatives.[16-19] Unfortunately, for the present derivative, the procedure yielded HBr-eliminated quinolinone **4.13** only.

As outlined in Scheme 2, abundant possibilities exist for electron delocalization within the bicyclic quinolinone core structure. The possibility of formation of the enol-form was used in a second strategy.

Quinolinone **4.4** was protected with either a tosyl group (**4.10a**) or an acetyl group (**4.10b**). In earlier studies, attempted formation of enamines from quinolinone **4.4** by keto-enolization was reported to succeed only after N-protection with an electron-withdrawing group like a tosyl group. An electron withdrawing group prevents formation of tautomer C (Scheme 2). For the current reaction scheme, tautomer C is not favorable, because obviously, reaction at the 3-position is less favorable in that state.[20, 21]
The protected quinolinones were enolized with LHMDS and trimethylsilylchloride to obtain enoxysilanes **4.14**.[22] In our hands, the formation of enoxysilanes proceeded smoothly at both protected quinolinone cores, without decomposition. This observation confirms the stabilizing contribution of the protective group.

In the subsequent step, the amino acid moiety was introduced by coupling of the enoxysilanes to imine **4.15**[23] (Scheme 5).

Scheme 5

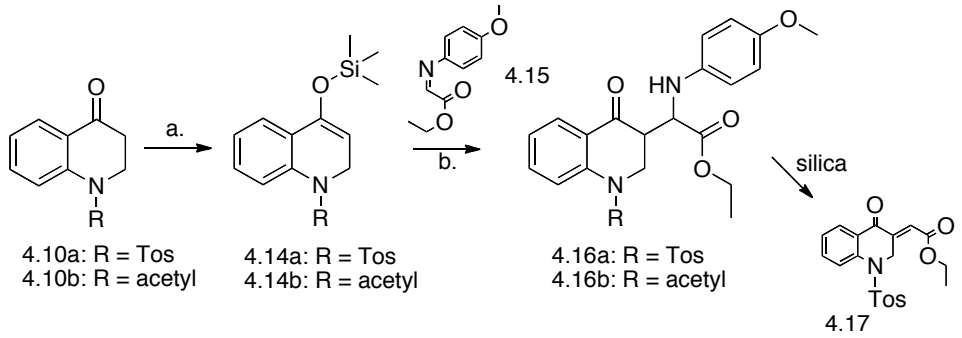

Reagents and conditions: a. LHMDS, TMSCl, THF, -80 °C; b. SmI_2, CH_2Cl_2.

The reaction is a SmI_2-catalyzed nucleophilic addition reaction.[24] The method had been applied successfully before to other bicyclic structures in our laboratory (see Chapter 3). Coupling products could be obtained for both **4.14a** and **b**. During purification of the product **4.16a**, the α-amine-eliminated compound **4.17** was formed, probably by decomposition on silica. Interestingly, no such amino-eliminated side-product was found in the acetylated series of compounds.

In earlier studies using similar methods, it was found that deprotection of the α-amino group with either iodobenzene diacetate[25] or ceric ammonium nitrate (CAN) and subsequent protection by acetylation yielded a stable intermediate. At

that stage, diastereomers could be separated easily by column chromatography or crystallization (see Chapter 3). The equivalent procedure for tosyl protected coupling product **4.16a** is shown in Scheme 6.

Scheme 6

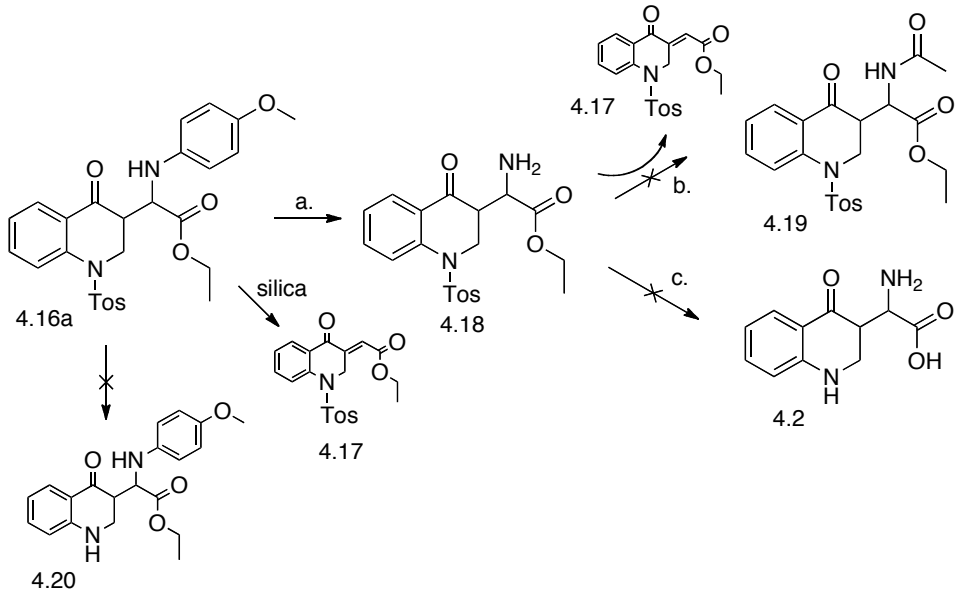

Reagents and conditions: a. CAN, ACN/H_2O; b. acetic anhydride, CH_2Cl_2; c. HCl.

For the current compound however, attempted acetylation after deprotection yielded no product but the deaminated compound **4.17**. The reason could be promotion of delocalization under the alkaline conditions used for the acetylation reaction. Attempts were made to isolate compound **4.18** and proceed from this point without further protection of the amino-group. Due to instability, compound **4.18** could not be purified sufficiently for full characterization. Only combination of partially elaborated analyses confirms the identity of the compound. In the ^{1}H NMR spectrum, a large singlet representing the tosyl-methyl protons can be seen clearly. In the ^{13}C NMR spectrum, clear signals are seen for the CH_3 groups of both the ethyl and the tosyl groups. In addition, signals are present for the two carbonylic carbon atoms (ketone and ester) and the remaining four aliphatic carbon atoms. Signals of atoms in the aromatic area are less well defined. Detection by mass spectrometry shows an m/z value that corresponds with the $(M+H)^+$ of the product. In the IR spectrum, the presence of a double peak at 3393-3331 cm^{-1} proves the presence of the primary α-

amino-group. The detection of ester (1735 cm^{-1}), ketone (1688 cm^{-1}) and sulfonylic (1165 cm^{-1}) peaks confirms the presence of the other functional groups in **4.18**.

To test the conditions needed for cleavage of the tosyl protective group from the quinolinone core, compound **4.10a** was deprotected. Using methods as described in literature[26], refluxing in concentrated HCl and acetic acid with a minor amount of water gave **4.4** in good yields. Therefore, partially purified **4.18** was subjected to hydrolysis under these conditions. Unfortunately, the harsh conditions caused severe decomposition for this intermediate. A mixture of at least 5 compounds was yielded. Analysis by mass spectrometry of the obtained mixture suggested the presence of components as shown in Scheme 7.

Scheme 7

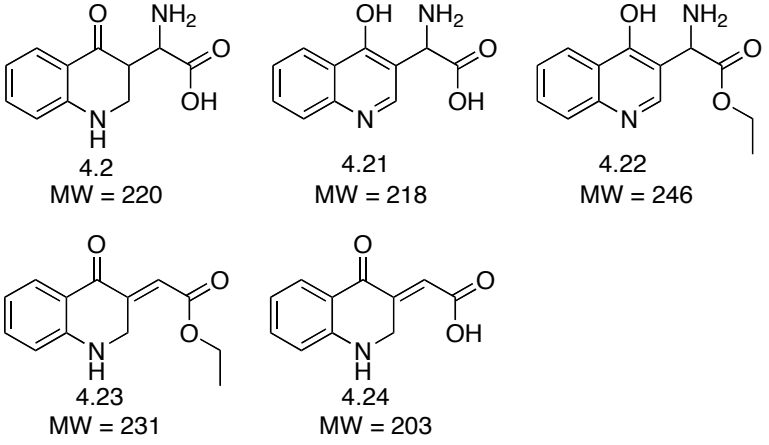

In the first place, as indicated by structures **4.21** and **4.22**, aromatization of the quinolinone core had occurred. Aromatization of the bicyclic system yields the energetically more favorable quinoline system. This seems to be feasible from quinolinone-tautomer B (Scheme 2), especially under the harsh conditions as applied during deprotection. In side-products **4.23** and **4.24**, the amino group is eliminated. This is analogous to α-amine-eliminated product **4.17**, which was formed during purification of **4.16a**.

In a last attempt in the tosyl-protected series, direct hydrolysis from **4.16a** to yield **4.20** was tested (Scheme 6). Again, only decomposition products were obtained from this reaction.

In contrast to **4.16a**, for derivative **4.16b**, deprotection and acetylation of the α-amino group proceeded without any difficulties (Scheme 8).

Scheme 8

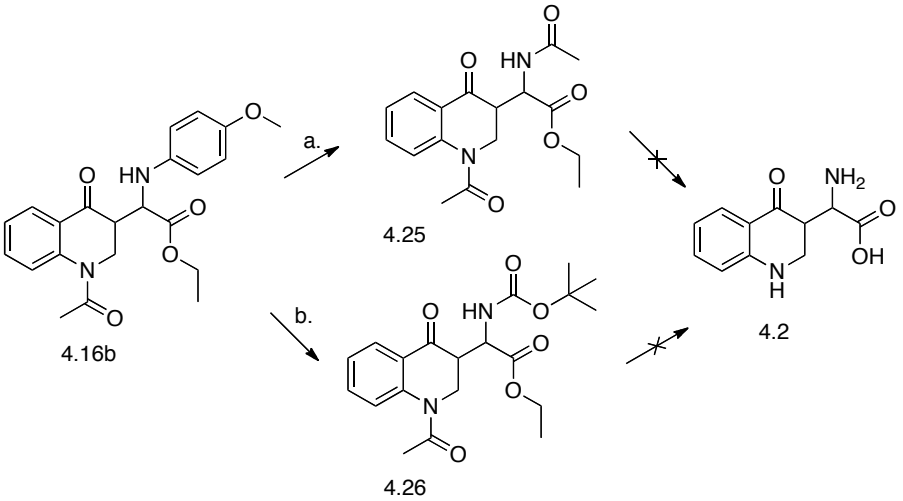

Reagents and conditions: a. (i) iodobenzene diacetate, MeOH (ii) acetic anhydride, CH_2Cl_2, K_2CO_3; b.(i) iodobenzene diacetate, CH_2Cl_2, (ii) Boc_2O, CH_2Cl_2, K_2CO_3.

For the deprotection of **4.16b**, reaction with iodobenzene diacetate was applied.[25] For subsequent protection of the α-amine, two protective groups were chosen. Following the previously developed general method, the amine was acetylated. Alternatively, the BOC protective group was employed. The BOC protective group could have two advantages for this compound. First, the physicochemical differences between the two diastereomers can be emphasized by the size of the group. If large groups are attached next to diastereocenters, the differences between the orientations are extended to a larger part of the molecule. This could facilitate the separation of the diastereomers. The second advantage of a BOC group over an acetyl group is the ease of cleavage of such a group. Whereas acetyl groups are cleaved under strongly alkaline or acidic conditions with heating, BOC cleavage can already be performed at mildly acidic conditions at ambient temperatures.

To our disappointment, diastereomers of neither **4.25** nor **4.26** could be separated. Moreover, again, cleavage of the acetyl protective groups from the quinolinone core of both compounds was problematic and gave many unwanted side-products.

Therefore, in a final attempt to synthesize **4.2**, BOC protective groups were chosen for protection of both the quinolinone core and for protection of the α-amino group after cleavage of the p-anisidino-group (Scheme 9).

Scheme 9

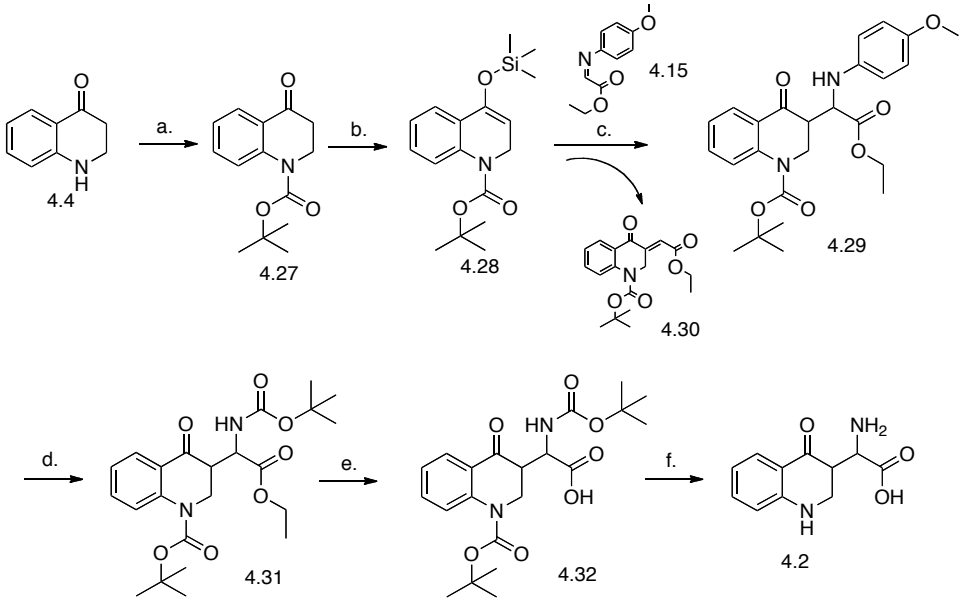

Reagents and conditions: a. Boc_2O, DMAP, THF; b. LHMDS, TMSCl, THF, -80 °C; c. SmI_2, CH_2Cl_2; d. (i) iodobenzene diacetate, MeOH, (ii) Boc_2O, CH_2Cl_2, K_2CO_3; e. KOH, $EtOH/H_2O$; f. TFA, CH_2Cl_2.

This approach proved to be successful. The BOC protective groups significantly improved the stability and ease of handling of all intermediates. After synthesis of **4.29**, diastereomers could be separated. Subsequent deprotection and BOC-protection yielded a mixture of diastereomers of **4.31**. Separation of the diastereomers was possible, but caused significant loss of product by decomposition on silica. Compound **4.31** was treated with KOH first to achieve ester hydrolysis. Although pure diastereomers of **4.31** were used, a mixture of **4.32** containing equal amounts of each diastereomer by HPLC was yielded. Keto-enolization explains the racemisation during hydrolysis. Under alkaline conditions, formation of the enol tautomer of the bicyclic structure is promoted by extraction of the slightly acidic proton at the β-position of the ring. The two diastereomers could be detected on silica-TLC by different colors of fluorescence but could not be separated by column chromatography. Therefore, the mixture

of all four stereoisomers was used in the next reaction step. Reaction with TFA in CH_2Cl_2 yielded **4.2** as a brightly yellow solid.

4.2.3 Synthesis of (4-oxo-1,2,3,4,-tetrahydroquinolin-3-yl)-acetic acid

Since BOC-protection of the quinolinone core structure had proven successful for the synthesis of **4.2**, this protective group was chosen again for the synthesis of **4.3**. The synthetic method is shown in Scheme 10.

Scheme 10

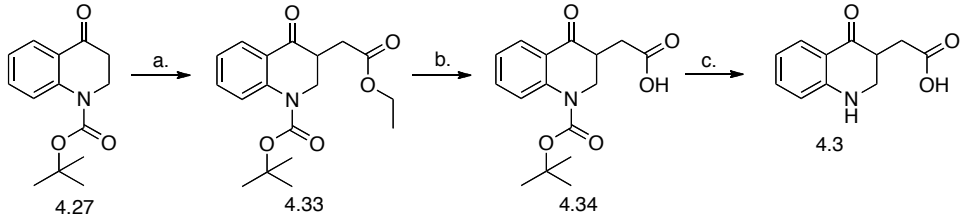

Reagents and conditions: a. 1. LHMDS, THF, -80°C, 2. Ethyl bromoacetate, THF, -80°C; b. NaOH, H_2O/EtOH; c. TFA, CH_2Cl_2.

In the first step, the protected quinolinone was enolized with LHMDS and the alkyl chain was introduced in the enol-intermediate by treatment with ethyl bromoacetate. Hydrolysis of the ethyl ester and subsequent BOC-deprotection of the bicyclic core yielded compound **4.3** in racemic form.

4.3 Enzyme inhibition

The final compounds **4.2** and **4.3** were tested for their ability to inhibit KAT, KYNase and KMO. Rat brain homogenate was used as the enzyme source for the KAT assay. Rat liver homogenates were used to assay activities of KYNase and KMO. Data for enzyme inhibition are shown in Table 1. As a reference, racemic ESBA ((*S,R*)-**4.35**) was tested. ESBA was the first published KAT II selective inhibitor.[18, 27]

Table 1 Enzyme inhibition

Compound	% KAT activity (inhibitor concentration)	% KYNase activity (inhibitor concentration)	% KMO activity (inhibitor concentration)
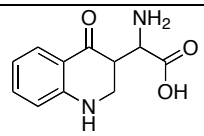 **4.2**	74.1±1.8 (3 mM)	92.9±1.2 (1 mM)	75.8±1.5 (1 mM)
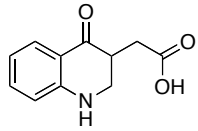 **4.3**	64.2±0.9 (3 mM)	17.4±0.4 (1 mM)	63.4±0.8 (1 mM)
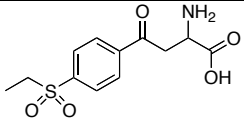 (*S,R*)-**4.35**	57.7±1.9 (1 mM) 44.7±1.6 (3 mM)	94.2±3.3 (1 mM) 74.5±2.8 (3 mM)	87.6±2.5 (1 mM) 85.6±1.3 (3 mM)

4.4 Conformational analysis and docking studies in kynureninase

Compounds **4.2** and **4.3** show pronounced differences in KYNase inhibitory activity (Table 1). To examine the origin of the observed differences, the energetically favorable conformations of these compounds in comparison with KYN and their interactions with KYNase were studied in more detail.

4.4.1 Structures

Structures that were used for the computational part of this work are shown in Scheme 11.

Scheme 11

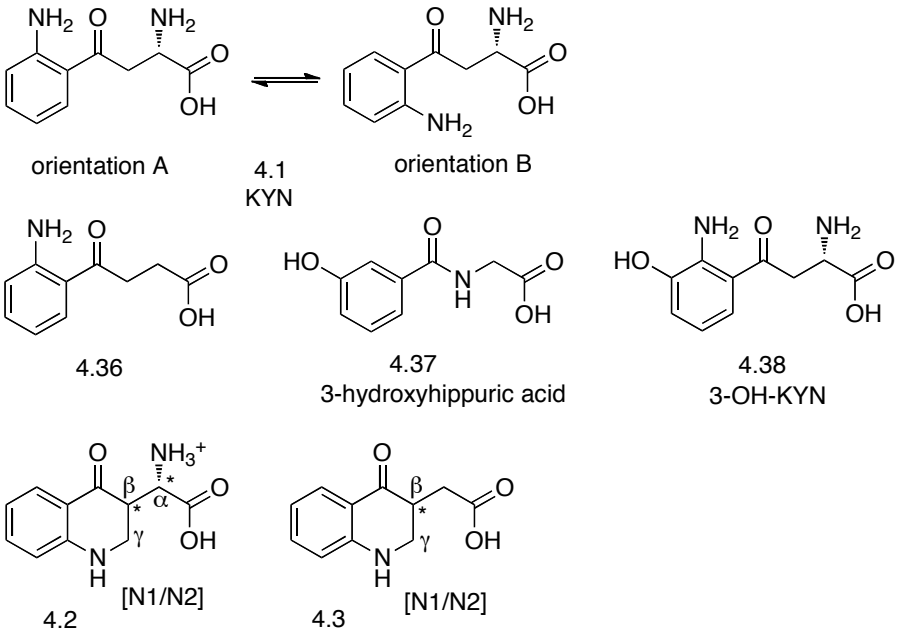

The key structure is KYN (**4.1**). The aromatic amino substituent of KYN can be oriented in two ways. In one orientation, arbitrarily named orientation A, the aromatic amino group and the benzoyl carbonyl group are oriented towards each other, implying the presence of an intramolecular H-bond. In an alternative orientation, arbitrarily named orientation B, the aromatic amino group is oriented into the opposite direction, away from the benzoyl carbonyl group. As depicted in Scheme 11, an equilibrium exists between both orientations.

Compound **4.36** is an equivalent of KYN, lacking the α-amino group. This compound showed inhibitory activity in the micromolar range for rat liver KYNase (data not shown).

Recently, the crystal structure of human KYNase in complex with 3-hydroxyhippuric acid (**4.37**), an analog of 3-OH-KYN (**4.38**), has become available.[28] Docking studies were performed in this crystal structure and **4.37** was used as the reference conformation for comparison of docked ligands. The aromatic nuclei in compounds **4.36**, **4.37** and **4.38** are represented in Scheme 11 in an orientation that corresponds with orientation A of KYN.

Compounds **4.2** and **4.3** were synthesized and tested in this study. For discussion of the structures, Cα, Cβ and Cγ positions are defined as shown in

Scheme 11. For the amino acid group in **4.2**, the Cα-*S*-enantiomers were taken into account only, because these enantiomers are most analogous to the naturally occurring enantiomer of KYN. For both **4.2** and **4.3**, the Cβ-*R* and Cβ-*S* enantiomers were studied. In addition to chiral centers, the directionality of the NH group in the bicyclic core was taken into account. Conformational analysis was performed with the NH-proton directed out of the plane (named N1) and towards the back of the plane (named N2). Most probably, at both the Cβ and the quinolinone NH positions, both forms, *R* and *S* or N1 and N2, respectively, are in continuous equilibrium. Since *in silico* methods do not take into account that the enantiomers/conformations are in equilibrium by tautomerization, the orientations need to be described and treated separately here.

4.4.2 Conformational analysis

To obtain insight into low energy conformations of KYN and the designed inhibitors, conformational analyses were performed. For KYN, both orientations A and B of the aromatic amino group were found during the conformational analysis with equal frequencies and equal conformational energies. The aliphatic side chain is fully extended in the low energy conformations.

The co-crystallized conformation of 3-hydroxyhippuric acid in the crystal structure of human KYNase[28] most probably reflects the binding orientation of KYN and 3-OH-KYN analogs. This conformation was used as a reference conformation adopted for binding to KYNase. Low energy conformations of KYN reflecting orientations A and B were superimposed on this conformation of 3-hydroxyhippuric acid.[28] Results are shown in Figure 1.

From the superposition it can be concluded, that the low energy conformations found for KYN highly resemble the conformation of KYNase bound 3-hydroxyhippuric acid. The superposition shows, that in orientation A of KYN, the aromatic amino group is oriented in between the aliphatic side chain and the phenolic OH-group of 3-hydroxyhippuric acid. In orientation B of KYN, the aromatic amino group is placed in a position that corresponds to the position para to the phenolic OH-group in 3-hydroxyhippuric acid.

Figure 1

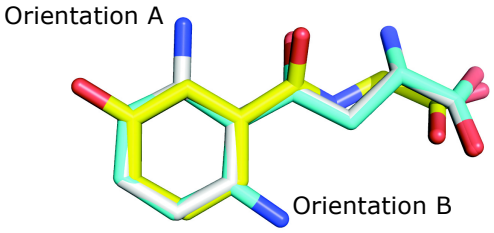

Superposition of KYN (orientation A: white and B: cyan) on 3-hydroxyhippuric acid (yellow).

To examine whether bicyclic structures **4.2** and **4.3** are likely to reflect energetically favorable conformations of KYN, conformational analysis of the structures was performed and resulting low energy conformations were compared to the conformations of KYN.

For all studied enantiomers, the bicyclic ring core structures were found to be merely planar. The planarity of the aromatic ring is extended over the carbonyl moiety and the NH-group. Some degree of flexibility is seen for the torsional angle C(=O)-Cβ-Cγ-N. Two distinct conformations were found for this angle, which can interconvert by ring inversion. This is shown in Figure 2 for *R*-**4.3**.

Figure 2

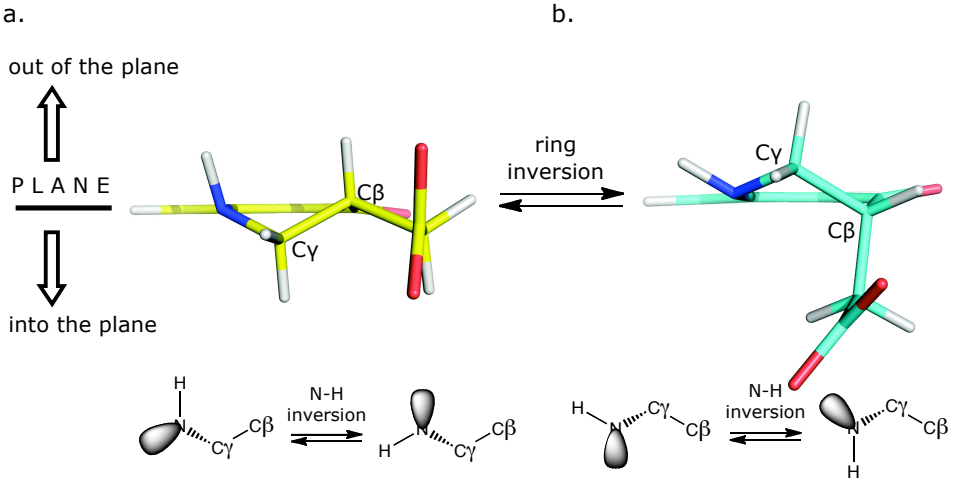

*Conformations of R-**4.3**, view along the plane of the bicyclic structure. (a) Cγ points into the plane, the carboxylate group is in an equatorial orientation. (b) Cγ points out of the plane, the carboxylate group is in an axial orientation.*

In Figure 2, the plane is defined by the aromatic core ring system. In one conformation (Figure 2a), the Cγ group points into the plane. Conversely, in the other conformation (Figure 2b), the Cγ atom points out of the plane. Since the bond from the carbonylic C-atom is in an sp2 state, the deviation from the plane of the Cβ atom is much less pronounced than the for the Cγ atom. In the case of Cγ pointing into the plane (Figure 2a), the Cβ has a slight deviation out of the plane. If Cγ points out of the plane (Figure 2b), the Cβ atom is oriented slightly into the plane. The orientation of the proton attached to the amino group has virtually no influence on the orientations of the C(=O)-Cβ-Cγ-N torsional angle but has by itself an equilibrium by N-H inversion between a semi axial and a semi equatorial position (Figure 2).
The orientation of the amino acid or carboxylate substituent in **4.2** and **4.3**, respectively, depends on the angle of the C(=O)-Cβ-Cγ-N torsion and the chirality at the Cβ atom. For example, for the *R*-enantiomer of **4.3** (Figure 2), if the Cγ-atom is oriented to point into the plane, the carboxylate substituent is oriented equatorially (Figure 2a). In contrast, if Cγ-atom is oriented to point out of the plane, the carboxylate substituent is oriented axially (Figure 2b). For the *S*-enantiomer, orientation of the Cγ-atom out of the plane corresponds to an equatorial orientation of the carboxylate substituent. Orientation of the Cγ-atom into the plane corresponds with an axial orientation of the carboxylate substituent.
The same pattern is observed for enantiomers of **4.2**. In most instances, a slight preference in terms of energy and numbers of unique low energy conformations was observed for equatorially substituted conformations. If an axially substituted conformation was found as the global minimum structure, this conformation was not taken into account for further studies. Instead, the most favorable conformation with an equatorially oriented side chain was chosen for these enantiomers. The energies found for the most favorable equatorial conformations differed just marginally from the global minimum energies.
It must be noted that due to free keto-enolization of the carbonyl bond, the distinct conformations of the bicyclic core structure described here in reality are easily interconvertible. Hence, during binding of the compounds to proteins, the most favorable conformation can be adopted relatively easily.

A database alignment was performed of all selected conformations of the enantiomers of **4.2** and **4.3**, KYN and 3-hydroxyhippuric acid. The aromatic core and the carboxylic acid moieties were chosen as templates for alignment. In Figure 3, results of the database alignment are shown.

Figure 3

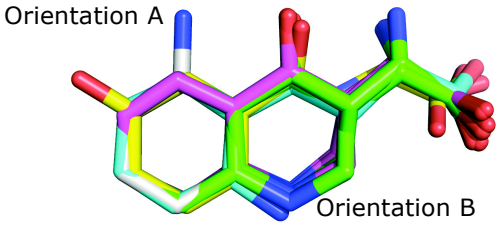

*Superposition of kynurenine (Orientation A: white and B: cyan), 3-hydroxyhippuric acid (yellow) and low energy conformations of **4.2** (green) and **4.3** (magenta).*

From the alignment it appears, that a good fit can be established of all aromatic and all carboxylate groups. Bicyclic compounds align in an orientation that corresponds to orientation B of KYN.

4.4.3 Docking in kynureninase

For docking studies, 3-hydroxyhippuric acid (**4.37**) was extracted from the crystal structure of human KYNase in complex with the inhibitor.[28] KYN and compounds **4.2**, **4.3** and **4.36** were docked into the active site of KYNase. Each molecule could be docked successfully.
The docked conformation of KYN, compared to the conformation of co-crystallized 3-hydroxyhippuric acid is shown in Figure 4.

Figure 4

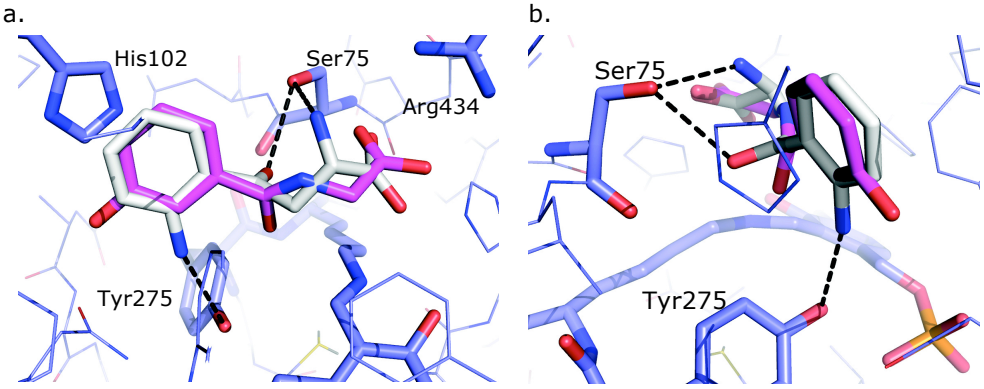

Overlay of docked KYN (white) and co-crystallized 3-hydroxyhippuric acid (magenta). (a) Front view and (b) side view.

KYN docks into the binding site in an orientation that is analogous to the orientation of 3-hydroxyhippuric acid (Figure 4a). The aromatic amino group is

oriented downwards and can interact by H-bond formation with Tyr275. The carboxylate group interacts with Arg434. Compared to the carbonyl group of 3-hydroxyhippuric acid, the KYN carbonyl group is oriented more towards the back to form a hydrogen bond with the side chain of Ser75 (Figure 4b). The α-amino group also interacts with the side chain of Ser75. As is shown in Figure 4b, although the orientation of the carbonyl group is not in the plane with the aromatic core, the relative orientation of the carbonyl and the aromatic NH_2 group represents orientation A as defined in Scheme 11.

To examine the influence of the α-amino group in KYN on the docked orientation of the molecule, compound **4.36** was docked into the KYNase binding site. The found orientation as compared to the orientation of KYN is shown in Figure 5. As appears from the figures, **4.36** docks in a conformation that is identical to the docked conformation of kynurenine. In the case of **4.36**, only the carbonyl group can interact with the side chain of Ser75.

After successful docking of kynurenine and **4.36**, experimental compounds **4.2** and **4.3** were docked into the crystal structure of human KYNase. In terms of docking energies, **4.2** and **4.3** docked equally well. Closer examination revealed some differences between the structures.
For compound **4.2**, β-*R* and β-*S* enantiomers were docked, with the NH group oriented in the N1 or N2 position. As stated earlier, there is a natural equilibrium between the two enantiomers by tautomerization and also between the orientation of the NH group in N1 or N2. The results found for docking of compound **4.2**, superimposed on docked KYN, are shown in Figure 6. For β-*R*-**4.2**, a convergent docking orientation was found for the N1 and N2 tautomers (Figure 6a). In this orientation, the aromatic moiety occupies a position that is slightly shifted downwards in the binding space compared to the aromatic moiety of KYN. As observed for the aromatic amino group of KYN, the heterocyclic NH-group interacts with the side chain OH group of Tyr275 by H-bond formation. Relative to KYN, the amino acid moiety of **4.2** is positioned higher in the binding space. The α-amino group points towards the opening in the binding site. Analysis of interactions with surrounding amino acid side chains showed, that the carboxylate group could still interact with Arg434 in this position. Furthermore, as observed for KYN, the α-amino group of **4.2** approaches Ser75 closely enough for H-bond formation (in the back of the plane, not shown in Figure 6).

Figure 5

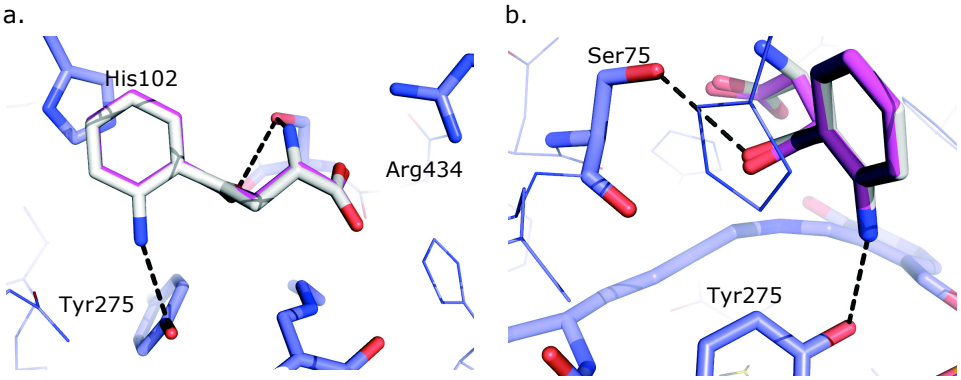

*Docked **4.36** (magenta) and KYN (white). (a) Front view and (b) side view.*

Figure 6

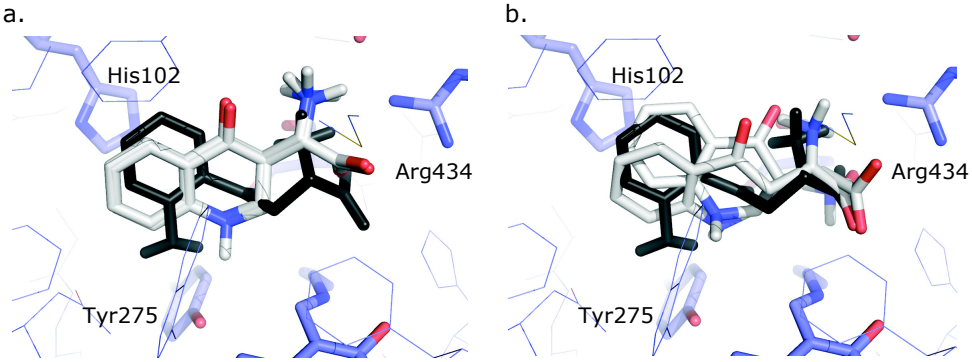

*Enantiomers of **4.2** (white) superimposed on KYN (black): (a) β-R-**4.2** and (b) β-S-**4.2**.*

Figure 7

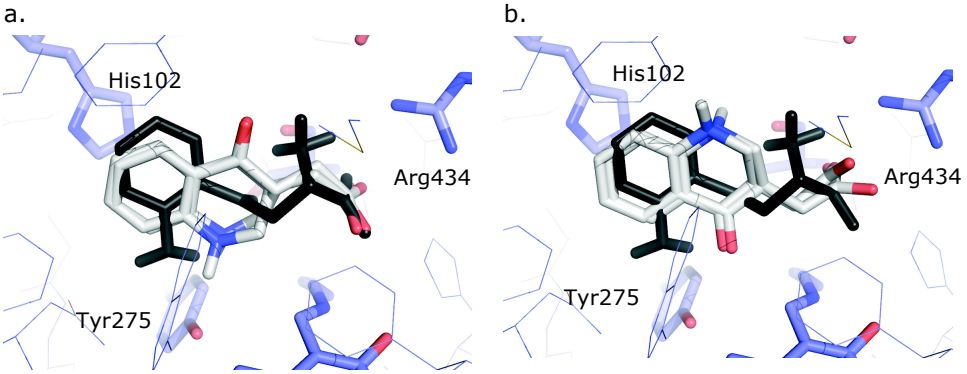

*(a) β-S- and β-R-**4.3** (white) superimposed on KYN (black) and (b) second orientation for R-enantiomers of **4.3** (white) superimposed on KYN (black).*

The orientation of the β-*S* tautomers (Figure 6b) is less well defined. The position of the carboxylate group is in accordance with the corresponding position of the KYN carboxylate group. The orientation of the quinolinone structure seems to be less optimal and is either in a higher or in a lower position than the aniline group of KYN. In the former case, if any, only weak hydrogen bonding between the nitrogen atom and the Tyr275 phenolic OH is possible.
In summary, docking positions are different for β-*R*-**4.2** and β-*S*-**4.2**. For the β-*R* tautomers, the orientation of the NH proton can be in either N1 or N2, without changing the position in the binding site. For the *β-S* tautomers, the optimal position of the conformation with the NH in an N1 orientation is different from the position of the conformation with the NH in the N2 orientation. This means that the *β-R* tautomers have more conformational freedom than the *β-S* tautomers. Therefore, it is to be expected that binding of **4.2** preferentially occurs in the *β-R* enantiomeric form. Overall, the conformational freedom of KYNase bound **4.2** is restricted by this preference.

For compound **4.3**, corresponding conformations were docked, reflecting the N1 and N2 orientation of the heterocyclic NH-group, and the *S* and *R* enantiomers at the β-carbon atom. Surprisingly, a convergent docking pose was found for all tautomeric forms of the molecule. This position, compared to KYN, is shown in Figure 7a. For the *R*-enantiomers, a second position was found, which is equally favorable (Figure 7b). For the *S*-enantiomers, a corresponding conformation was found with a slightly less favorable orientation of the carboxylic side chain (not shown).
As is apparent from Figure 7a, in the first docked pose, the position of the quinolinone NH atom of **4.3** approaches the position of the corresponding atom in KYN. The carbonyl moiety points upwards, out of the binding site. The bicyclic compound occupies a space that corresponds well with the binding space of KYN. In particular, the carboxylate group is oriented in an identical position, favoring salt bridge formation with Arg434. Analysis of H-bonding interactions revealed, that the heterocyclic nitrogen atom interacts with the phenolic OH group of Tyr275. The aromatic ring system is in a position favorable for hydrophobic interactions with His102. In the second orientation, the bicyclic system is 'mirrored'. The carbonyl group points down and interacts with Tyr275. Again, the carboxylate group is in a position that allows salt bridge formation with Arg434. The convergent orientations of all enantiomers and tautomers of this molecule suggest, that the docking space does not prevent the compound from free tautomerization from one enantiomer to the other and back and from free ring

inversion with the NH oriented in the N1 or N2 position. This is in contrast to **4.2**, for which docking positions differ for the tautomers and docking in the *β-R* tautomeric form is clearly preferred over the *β-S* tautomeric form.

4.5 Discussion and conclusion

In the present work, the synthesis of conformationally restricted KYN analogs is presented. The molecules were tested for their ability to inhibit key kynurenine pathway enzymes. Interactions of the molecules with KYNase were further explored by conformational analysis and docking studies.

4.5.1 Compound design and *in vitro* activity

Conformational restriction of molecules is a powerful tool to study the properties of ligands as favored by the target proteins. In the ideal case, a ligand is restricted in a conformation that reflects the conformation when bound to the target protein. This results in a lower energy barrier towards binding, causing enhanced affinity for the target. Furthermore, enhanced selectivity for the desired target can be achieved by conformational restriction.
In the present case, inhibition of KAT is desired. The compounds should inhibit KAT selectively over KYNase and KMO to achieve a decrease in brain KYNA levels *in vivo*. Compared to reference inhibitor (*S,R*)-**4.35**, KAT inhibitory activity of **4.2** and **4.3** in the performed enzyme assays is limited. Apparently, the introduction of the aliphatic ring in the structure causes a conformational restriction that is not optimal for interaction with KAT. Still, species differences exist in KATs, and inhibition should be tested in assays using alternative enzyme sources.
Liver KMO is inhibited moderately well by **4.2** and **4.3**. After systemic administration, the effects of the compounds on liver enzymes are likely to most pronouncedly define the overall effect of the molecules. Therefore, in the ideal situation, inhibitory activity for KMO should be absent in KAT selective inhibitors.
The most striking finding of this study is the difference between **4.2** and **4.3** in inhibition of KYNase. At a bath concentration of 1 mM, amino acid **4.2** shows virtually no inhibitory activity. In contrast, carboxylic acid analog **4.3** inhibits the enzyme to 17 % of its original activity at the same bath concentration.

Conformational analyses and docking experiments using the crystal structure of human KYNase were performed to understand the large difference in KYNase inhibitory potency between the structurally very similar compounds **4.2** and **4.3**.

For the discussion of the results, it should be noted, that in the present study, inhibition of this enzyme is disfavored.

4.5.2 Conformational analysis

Conformational analysis of KYN showed, that the compound adopts either one of two defined low energy conformations, referred to as orientations A and B. In both orientations, the aliphatic side chain is fully extended. The superposition on 3-hydroxyhippuric acid (Figure 1) reveals that the energetically favorable conformations of KYN and the conformation of 3-hydroxyhippuric acid bound to human KYNase align well. 3-Hydroxyhippuric acid was designed as a structural analog of 3-OH-KYN (**4.38**, Scheme 11). The aromatic OH-group of 3-hydroxyhippuric acid corresponds to the 3-OH group in 3-OH-KYN. In the superposition, the aromatic amino group of KYN in orientation A is located in the position that would be accommodated by the aromatic NH_2 of 3-OH-KYN, in between the aromatic OH and the aliphatic chain substituent (see Scheme 11). Therefore, from the current superimposition it can be concluded that the conformation of 3-hydroxyhippuric acid bound to KYNase corresponds to orientation A rather than orientation B of KYN. Interestingly, crystal structures of KAT II in complex with kynurenine[29] show, that the preferred conformation of KYN for interaction with KAT II more closely resembles orientation B than orientation A.

Compounds **4.2** and **4.3** were designed as potential selective KAT inhibitors. The compounds are KYN analogs, locked in orientation B by introduction of a methylene bridge between the Cβ of the aliphatic side chain and the aromatic NH_2 group. Conformational analysis showed that different orientations of the Cγ atom in combination with the substitution pattern at Cβ result in an axial or equatorial orientation of the amino acid or carboxylate ring substituent (Figure 2). Due to the possibility of tautomerization at the carbonyl group and consequent racemisation at Cβ, all conformations found for **4.2** or **4.3** are in constant equilibrium under natural conditions. Therefore, conformational energies merely reflect the relative preferences or percentage of time for a molecule to be in a certain conformation. Energy barriers between the conformations are relatively low and unless restricted by environmental factors like enzyme binding, the conformation of the molecule is changing constantly and freely from one conformation to another. The flexibility of the molecules caused by the tautomerization might be favorable for finding the correct binding conformation in the enzyme. This might enhance the binding affinity.

The structures **4.2** and **4.3** represent energetically favorable conformations of KYN. Superposition of the compounds with KYN and 3-hydroxyhippuric acid (Figure 3) shows, that the compounds indeed align most favorably in a way representing orientation B of KYN (Scheme 11). This means, that theoretically, binding to KYNase is less favorable for these conformationally restricted analogs than for KYN. Accordingly, compound **4.2** lacks KYNase inhibitory potency (Table 1). Unexpectedly however, compound **4.3** inhibits KYNase much more potently than KAT II. To find a probable explanation for this observation, docking studies in KYNase were performed.

4.5.3 Docking

4.5.3.1 Docking of kynurenine

First, the docked position of KYN in KYNase was examined and compared to co-crystallized 3-hydroxyhippuric acid. Binding of KYN to the binding site of KYNase is a dynamic process. KYNase is a pyridoxal 5'-phosphate (PLP) dependent enzyme. The co-enzyme PLP facilitates the catalytic process. In the resting state of the enzyme, the co-enzyme is bound to the side chain of a lysine residue in the active site in a so-called internal aldimine linkage. During binding of the substrate in the catalytic site, the internal aldimine linkage is broken and an external aldimine is formed with the α-amino group of the substrate. For proper positioning of the incoming substrate, a strictly conserved interaction between the side chain carboxylate group of the ligand and a conserved Arg residue is crucial. In human KYNase, the Arg residue is Arg434.[28, 30]

Overall, KYN fits well in the docking space. The ligand adopts an orientation that is equivalent to the orientation of co-crystallized 3-hydroxyhippuric acid (Figure 4). The aromatic moiety of KYN aligns with the aromatic ring of the co-crystallized ligand. As expected, the aromatic amino group is oriented in a way reflecting orientation A. The KYN carboxylate group points towards Arg434.

In the catalytic cycle, after formation of the aldimine link between the cofactor and KYN, the β-γ bond of the substrate is catalytically broken. This reaction is initiated by formation of a tetrahedral gem-diolate intermediate around the carbonyl C-atom. Based on the crystal structure of KYNase in complex with 3-hydroxhippuric acid, it was hypothesized that Ser75 has a key role in stabilization of this gem-diolate intermediate. Additionally, Tyr275 is involved in stabilization.[28] In the docked conformation of KYN, the benzoylic carbonyl group points towards the side chains of Ser75 and Tyr275. As for 3-hydroxyhippuric acid, this reflects the role of these residues in the catalytic mechanism.

In the present results, the α-amino group of KYN points upwards, towards the opening of the binding site, rather than towards PLP. This is not an orientation that would be expected based on the mechanistic properties of the enzyme. For proper interaction with the co-enzyme, the α-amino group should be oriented towards the PLP aldimine bond, to participate in transaldimination for formation of the external aldimine bond with the co-enzyme.[31, 32] Therefore, the orientation of the group in docked KYN does not reflect the natural situation. This discrepancy can be explained by the rigidity of the model. In the dynamic process of binding, the incoming KYN enforces the hydrolysis of the internal aldimine and formation of the external aldimine bond accommodating the α-amino group. In the docking experiment, the internal aldimine bond cannot be hydrolyzed to make space for this group. Instead, the amino group is forced into an unoccupied area in the binding space. Apparently, this space is available in the access channel of the enzyme.

Although the α-amino group is important for covalent interaction of substrate and co-enzyme, binding affinity is determined by interaction of the entire substrate molecule in the binding pocket. To examine whether the overall conformation of the remainder of the molecule is directed by the orientation of the α-amino group, des-amino KYN **4.36** was docked into KYNase. As is shown in Figure 5, the docked conformation of **4.36** is identical to the conformation of KYN. From these results, it can be concluded that that binding of the remaining part of the molecule does not depend on the orientation of the α-amino group. In contrast, it is postulated that the orientation of the α-amino group is directed by salt bridge formation of the carboxylate group with Arg434 on one hand and the hydrophobic interactions of the aromatic core on the other hand. Consequently, the α-amino group is pushed towards the cofactor and formation of the external aldimine bond is enforced. For the present docking results, this means that, although the orientation of the α-amino group is not correct, the remainder of the molecule is docked correctly, reflecting the bound orientation of KYN in human KYNase. Binding of the aromatic and the carboxylate moieties to the binding site of KYNase can be seen as the first step in initiation of the catalytic cylce.

*4.5.3.2 Docking of **4.2** and **4.3***

Based on the results discussed above, for the discussion of the docking results of compounds **4.2** and **4.3**, two anchor points of ligand-enzyme interaction can be defined. The first anchor point is defined by the position of the aniline moiety of the molecule. For KYN and **4.36**, the aromatic ring is involved in π-stacking with

His102. The aromatic amino group points down towards the side chain of Tyr275. The second anchor point is formed by the carboxylate group, which interacts with Arg434 in a salt bridge. The preferred binding mode of a ligand is defined by the optimal position of both anchor points in the binding site.

In terms of scoring results, all conformations of compounds **4.2** and **4.3** docked with comparable affinities in the crystal structure of KYNase. Upon closer inspection of orientations, some differences were found between binding of **4.2** and **4.3** that could account for differences in *in vitro* inhibitory activity. Obviously, the differences are caused by the presence of the α-amino group in **4.2** and the absence of this group in **4.3**.
For compound **4.2**, a defined binding orientation was found for the *R*-enantiomers (Figure 6a). The orientation is irrespective of the orientation of the quinolinone NH proton. In this orientation, the quinolinone amino group is oriented towards Tyr275. The carboxylate group forms salt bridges with the side chain of Arg434, but in a position that is not as optimal as adopted by the carboxylate moiety of KYN. The *S*-enantiomers are positioned differently. For the *S*-enantiomers, the carboxylate group is oriented for good interaction with Arg434 (Figure 6b). However, here the position of the aromatic moiety seems to be forced into suboptimal orientations compared to the orientation of the aniline moiety in KYN. Apparently, conformational restriction forces the molecule into positions in which either the aromatic ring or the carboxylate moiety is oriented sub-optimally for interaction with the enzyme. As discussed above, tautomerization allows free racemization from one enantiomer to the other. Since apparently, the *R*-enantiomer docks in a preferred orientation in KYNase, the molecule is driven to be in that enantiomeric form. This can be seen as a restriction of conformational freedom of the enzyme bound molecule. In terms of entropy, the restriction is a factor of loss of entropy during ligand-enzyme binding. Since loss of entropy is disfavored, this has a negative effect on binding affinity.
In contrast, for compound **4.3**, two defined orientations were found that could both be adopted by both enantiomers, irrespective of the orientation of the quinolinone NH proton. In the first orientation, the quinolinone amino group points down towards Tyr275 (Figure 7a). In the second orientation, the ring is mirrored. In this way, the carbonyl group of the quinolinone core points down towards Tyr275. The amino group points up. In either orientation, the caboxylate group is in a position that is optimal for interaction with Arg434. Therefore, in contrast to **4.2**, all enantiomers and tautomers of **4.3** can adopt

either of 2 orientations, both of which allow for (almost) optimal interaction of both anchor points within the KYNase binding site. For the bound molecule, the interconversion from one enantiomer to the other is not restricted. This means that the loss of entropy due to tautomeric restriction as seen for **4.2** does not apply for **4.3**. Thus, total entropy and hence binding affinity is improved compared to **4.2**, allowing for stronger competition with KYN for binding to the enzyme. This could explain the pronounced inhibition of KYNase by **4.3** as observed *in vitro*.

It must be noted that the orientation of the α-amino group in **4.2** is upwards, away from PLP in all docked conformations. Similar to what was discussed for kynurenine, this could represent and artefact, caused by the rigidity of the internal aldimine bond in the docking experiment. Theoretically, the compound could act as a covalent inhibitor by formation of an external aldimine link with PLP. This possibility cannot be ruled out by the presented data. However, based on such mechanisms, an enhanced KYNase inhibitory potency compared to **4.3** would be expected *in vitro*. Therefore, the possibility of covalent interaction of **4.3** with the enzyme is not further taken into account.

4.5.4 Summary and conclusion

In summary, this work explores the effects of conformational restriction of KYN in one of its energetically favorable conformations. Whereas desired KAT inhibitory activity seems to be limited in the assays used here, the conformational restriction has important effects on inhibition of KYNase. As explained by molecular docking studies, introduction of the restriction in amino acid analog **4.2** impedes optimal binding of the molecule in the KYNase catalytic site. This shifts selectivity of the compound towards KAT inhibition, rather than KYNase inhibition. In contrast, due to the lack of the α-amino group in conformationally restricted analog **4.3**, this compound can adopt positions that are optimal for both binding of the aromatic amino group and the carboxylate group, irrespective of the chirality at the Cβ atom. Therefore, KYNase inhibitory activity is much more pronounced for this compound than in **4.2**.
Overall, due to lack of pronounced potency and selectivity for inhibition of KAT if compared to potency towards KMO and KYNase, the molecules presented here are expected to have an increasing rather than a decreasing effect on brain KYNA levels *in vivo*. Compound **4.3** in particular will cause increased levels of KYN in the periphery by inhibition of metabolism of this key intermediate by liver KYNase. KYN will cross the blood brain barrier. This will result in elevated levels

of this KAT substrate in the brain. Enhanced turnover into KYNA will finally result in elevated levels of this metabolite in the brain.

In conclusion, the present study did not result in the design of the desired selective KAT inhibitors. However, insight was gained into properties in the KYNase binding site, which can be used in the search for selective inhibitors of KAT or KYNase. For future studies on inhibitory activity and selectivity of compounds, the availability of crystal structures of KMO could be of major importance. Until then, more work should be done on the characterization of differences between KAT and KYNase and differences for each enzyme amongst different species.

4.6 Experimental section

General NMR spectra were taken on a Varian spectrometer, at the frequency as stated in the text. Chemical shifts are given in ppm. The splitting patterns are designated as follows: s = singlet, d = doublet, t = triplet, m = multiplet, bs = broad singlet. Coupling constants are given in hertz (Hz). IR spectra are taken on an ATI-Mattson spectrophotometer. GCMS analysis were performed on a Shimadzu GCMS-QP500 system equipped an AOC-20i auto injector and a CP-Sil 5 CB column (15m x 0.25mm; 0.10µm film thickness). Mass spectra (ESI) were taken on an API 3000 MS/MS system. Accurate mass measurements (HRMS) were performed using a flow injection method on a LTQ-Orbitrap XL mass spectrometer (Thermo Electron, Bremen, Germany) with a resolution of 60000 at m/z 400. All final compounds had ad least 95% purity, as determined by HPLC. Solvents and reagents were obtained from general sources and used as such. THF was dried by distillation over Na.

3-Phenylaminopropionic acid methyl ester (4.7)
A mixture of aniline (**4.5**, 5.01 g, 53.8 mmol), methyl acrylate (**4.6**, 5.4 mL, 5.16 g, 60 mmol) and acetic acid (0.5 mL) was stirred at 80 °C overnight. Vacuum distillation (95 °C, 0.03 mbar) yielded 7.17 g (74 %) of **4.7** as a yellow solid.
^{1}H NMR (200 MHz, $CDCl_3$) δ 2.60-2.66 (t, 2H, CH_2), 3.4-3.49 (t, 2H, CH_2), 3.70 (s, 3H, CH_3), 6.60-6.77 (m, 3H, ArH), 7.15-7.26 (m, 2H, ArH) ppm; ^{13}C NMR (50 MHz, $CDCl_3$) δ 171.3, 146.0, 127.9, 116.3, 111.6, 50.2, 37.9, 32.2 ppm; IR (KBr) 3401, 2951, 1733, 1603, 1508, 1175, 751, 694 cm^{-1}; GCMS m/z 179 (M).

3-[Phenyl-(toluene-4-sulfonyl-amino)-propionic acid methyl ester (4.8)
3-Phenylaminopropionic acid methyl ester (**4.7**) (2.01g, 11.2 mmol) was dissolved in pyridine (20mL). p-Toluene-sulfonyl chloride (2.33g, 12.2 mmol) was added portionwise. A precipitate appeared after several minutes, stirring the mixture at r.t.. After 15 minutes, the mixture was heated at reflux for one hour. The mixture was then left to cool to r.t., and water was added. The mixture was extracted with diethyl ether. The combined organic layers were washed with 4N HCl, 1N NaOH, water, and brine, dried ($MgSO_4$), filtered and the solvent was evaporated. A yellow oil (3.46, 93%) was obtained, which was used in the subsequent reaction without further purification.
^{1}H NMR ($CDCl_3$) δ 2.42 (s, 3H, TOS-CH_3), 2.51-2.59 (t, 2H, *J*=7.63, 7.35Hz, NCH_2CH_2), 3.59 (s, 3H, $COOCH_3$), 3.80-3.87 (t, 2H, *J*=7.64, 7.34Hz, NCH_2), 7.00-7.05 (m, 2H, ArH), 7.22-7.32 (m, 4H, ArH), 7.45-7.50 (d, 2H, ArH) ppm; ^{13}C NMR ($CDCl_3$) δ 171.7, 143.8, 139.2, 135.2, 129.7, 129.4, 129.1, 128.4, 128.0, 52.0, 47.0, 34.2, 21.8 ppm; IR (NaCl) 2951, 1738, 1349, 1163, 697, 654 cm^{-1}; GCMS m/z 333 (M).

3-[Phenyl-(toluene-4-sulfonyl)-amino]-propionic acid (4.9)
3-[Phenyl-(toluene-4-sulfonyl-amino)-propionic acid methyl ester (**4.8**) was dissolved in MeOH (20 mL), and 10% KOH in H_2O(7.5 mL) was added. The mixture was stirred at r.t. overnight. The methanol was evaporated, and the aqueous layer was washed with CH_2Cl_2. The aqueous layer was then acidified with 4N HCl, and extracted with CH_2Cl_2. The organic extracts were merged, dried ($MgSO_4$), filtered, and the solvent was evaporated. A white solid was yielded (2.87 g, 87 %).
^{1}H NMR ($CDCl_3$) δ 2.42 (s, 3H, $ArCH_3$), 2.55-2.63 (t, 2H, CH_2), 3.79-3.87 (t, 2H, CH_2), 7.01-7.06 (m, 2H, ArH), 7.26-7.34 (m, 5H, ArH), 7.45-7.50 (m, 2H, ArH) ppm; ^{13}C NMR ($CDCl_3$) δ 174.8, 142.2, 137.4, 133.4, 128.0, 127.7, 127.4, 126.8, 126.3, 44.9, 32.2, 20.1 ppm; IR (KBr) 3051, 2922, 1703, 1349, 1159, 1094, 571 cm^{-1}.

2,3-Dihydro-1H-quinolin-4-one (4.4)
Polyphosphoric acid (17 g) was heated to 100°C. 3-[Phenyl-(toluene-4-sulfonyl)-amino]-propionic acid (**4.9**, 1.81 g, 5.67 mmol) was added. The mixture (orange solution) was stirred at 100 °C for 1.25 h, and was then quenched by the addition of ice. The aqueous suspension obtained was brought to alkaline pH with 4 N NaOH and extracted with Et_2O. The combined organic layers were washed with brine, dried ($MgSO_4$), filtered, and the solvent was evaporated. A yellow oil was obtained (0.6245 g, 75 %).
^{1}H NMR (200 MHz, $CDCl_3$) δ 2.64-2.71 (t, 2H, CH_2), 3.5-3.58 (t, 2H, CH_2), 4.47 (bs, 1H, NH), 6.64-6.75 (m, 2H, ArH), 7.23-7.32 (m, 1H, ArH), 7.80-7.85 (dd, 1H, ArH) ppm; ^{13}C NMR (50 MHz, $CDCl_3$) δ 192.4, 150.7, 133.7, 126.1, 117.8, 116.3, 114.4, 40.7, 36.6 ppm; IR (NaCl) 3353, 2965, 2823, 1667, 1607, 1511, 1341, 1239, 1152, 761 cm^{-1}; GCMS m/z 147 (M).

1-(Toluene-4-sulfonyl)-2,3-dihydro-1H-quinolin-4-one (4.10a)
To a mixture of 2,3-dihydro-1H-quinolin-4-one (**4.4**, 1.46 g, 9.92 mmol) in pyridine (20 mL), p-toluenesulfonyl chloride (2.07 g, 10.8 mmol) was added. The mixture was stirred at r.t. for 25 minutes. Then, the mixture was placed on an oil bath preheated to 95 °C, and was stirred at that temperature for 1.25 h. The mixture was left to cool to r.t.. Water was added, and the aqueous layer was extracted with CH_2Cl_2. The combined organic extracts were washed with 4 N HCl, 1 N NaOH, and brine, dried ($MgSO_4$), filtered, and the solvent was evaporated. Recrystallization from EtOAc/Hex yielded 1.74 g (58%) brownish crystals.
^{1}H NMR (200 MHz, $CDCl_3$) δ 2.34-2.41 (s and t, 5H, CH_2 and CH_3), 4.19-4.25 (t, 2H, CH_2), 7.20-7.30 (m, 3H, ArH), 7.52-7.61 (m, 3H, ArH), 7.84-7.95 (2H, 2H, ArH) ppm; ^{13}C NMR (50 MHz, $CDCl_3$) δ 191.2, 143.1, 140.8, 135.3, 133.2, 128.6, 126.2, 125.4, 124.2, 124.1, 123.1, 44.7, 35.0, 20.1 ppm; IR (KBr) 1681, 1596, 1474, 1456, 1351, 1294, 1163, 830, 774, 731, 684 cm^{-1}; GCMS m/z 301 (M).

3-Bromo-1-(toluene-4-sulfonyl)-2,3-dihydro-1H-quinolin-4-one (4.11)
To a solution of 1-(toluene-4-sulfonyl)-2,3-dihydro-1H-quinolin-4-one (**4.10a**, 0.150 g, 0.498 mmol) in dry $CHCl_3$ (2.5 mL), a solution of Br_2 (78.0 mg, 0.488 mmol) in $CHCl_3$ (2.5 mL) was added. The mixture was heated at reflux for 3 hours. After cooling to room temperature, the solvent of the mixture was evaporated. Column chromatography (silica, petroleum ether 40-60:EtOAc 4:1) gave a slightly green viscous oil (0.155 g, 82%).
^{1}H NMR (200 MHz, $CDCl_3$) δ 2.41 (s, 3H, CH_3), 4.31-4.63 (m, 3H, CH_2 and CHBr), 7.21-8.03 (m, 8H, ArH) ppm; ^{13}C NMR (50 MHz, $CDCl_3$) δ 143.6, 134.8, 133.9, 128.7, 127.7, 125.6, 123.9, 121.2, 120.9, 51.1, 44.3, 20.1 ppm; IR (NaCl) 3066, 2924, 1691, 1597, 1474, 1354, 1287, 1164, 1092, 898, 760, 676 cm^{-1}.

Attempted synthesis of 2-acetylamine-2-[4-oxo-1-(toluene-4-sulfonyl)-1,2,3,4-tetrahydroquinolin-3-yl]-malonic acid diethylester (4.12), yielding 1-(toluene-4-sulfonyl-4(*1H*)-quinolinone (4.13)

Attempted synthesis of **4.12**, using a procedure as described in ref[16] gave the HBr eliminated product **4.13**.

^{1}H NMR (200 MHz, $CDCl_3$) δ 2.38 (s, 3H, $TosCH_3$), 6.36-6.40 (d, *J*=8.54Hz, 1H, COCH=CH), 7.26-7.41 (m, 3H, ArH), 7.52-7.61 (dt, 1H, ArH), 7.73-7.76 (dd, *J*=6.6, 1.7 Hz), 8.15-8.19 (m, 1H, ArH), 8.29-8.34 (m, 1H, ArH), 8.53-8.57 (d, *J*=8.55, 1H, COCH=CH) ppm; ^{13}C NMR (50 MHz, $CDCl_3$) δ 177.0, 144.9, 136.4, 135.4, 132.3, 131.2, 128.9, 128.6, 126.9, 1260, 125.7, 124.9, 124.1, 116.7, 111.0, 20.2 ppm; IR (KBr) 3080, 2925, 1640, 1600, 1467, 1369, 1169, 1080, 1034, 953, 675 cm^{-1}; GCMS m/z 299 (M).

1-Acetyl-2,3-dihydro-1H-quinolin-4-one (4.10b)

A solution of 2,3-dihydro-1H-quinolin-4-one (**4.4**, 0.944 g, 6.42 mmol) and triethylamine (1.9 mL, 1.4 g, 14 mmol) in dry CH_2Cl_2 (20 mL) under an atmosphere of N_2 was cooled on ice. Acetylchloride (1 mL, 14 mmol) in CH_2Cl_2 (5 mL) was added dropwise over 15 minutes. The mixture was left to stir at 0 °C for 5 minutes, and was then left to warm to room temperature. After stirring at r.t. for 1 hour, water was added to quench the reaction. The layers were separated, and the aqueous layer was extracted with CH_2Cl_2. The combined organic layers were washed with brine, dried ($MgSO_4$), filtered, and the solvent was evaporated. Purification by column chromatography (silica, petroleum ether:EtOAc 4:1 → 1:1) yielded 0.62 g (48%) of a brightly yellow solid.

^{1}H NMR (200 MHz, $CDCl_3$) δ 2.34 (s, 3H, $AcCH_3$), 2.77-2.83 (t, 3H, CH_2), 4.21-4.27 (t, 2H, CH_2), 7.24-7.31 (m, 1H, ArH), 7.41-7.45 (bd, 1H, ArH), 7.52-7.59 (t, 1H, ArH), 7.99-8.03 (d, *J*=7.63, ArH) ppm; ^{13}C NMR (50 MHz, $CDCl_3$) δ 192.5, 167.8, 142.5, 132.6, 126.3, 124.6, 124.1, 122.6, 42.5, 38.0, 21.6 ppm; IR (KBr) 2949, 1690, 1649, 1599, 1475, 1383, 1265, 1206, 1092, 1001, 849, 770 cm^{-1}; GCMS m/z 189 (M)

Reaction with acetic anhydride and triethylamine in CH_2Cl_2 at r.t. gave the product in 40 % yield.

General method for the preparation of 1-protected 4-trimethylsilanyloxy-1,2-dihydroquinolines

1-(Toluene-4-sulfonyl)-4-trimethylsilanyloxy-1,2-dihydroquinoline (4.14a)

A solution of 1-(toluene-4-sulfonyl)-2,3-dihydro-1H-quinolin-4-one (**4.10a**, 0.480g, 1.59 mmol) in dry THF (14 mL) was cooled to -78°C under N_2. A solution of LHMDS (0.410g, 2.45 mmol) in dry THF (2 mL) was added. The glassware was rinsed with another 1 mL dry THF. The mixture was left to warm up to -5°C over 1 hour. The mixture was then cooled to -78°C, and TMSCl (0.31mL, 0.26g, 2.39 mmol) was added in one portion. The mixture was left to slowly warm up, stirring under N_2. After 1h (temperature 0°C), water was added. The mixture was extracted with EtOAc (3x). The combined organic layers were washed with NH_4Cl sat aq., dried ($MgSO_4$), filtered, and the solvent was evaporated. 0.614 g of an orange solid was obtained, which was used for the next reaction without purification.

IR (KBr) 2960, 1642, 1352, 1248, 1165, 1068, 874, 846, 768, 669 cm^{-1}; GCMS m/z 373 (M), 301 (M-Me_3Si).

1-(4-Trimethylsilanyloxy-2H-quinolin-1-yl)-ethanone (4.14b)

IR (NaCl) 3322, 2957, 1692, 1644, 1600, 1483, 1335, 1245, 1212, 1083, 872, 759 cm^{-1}.

(4-Methoxy-phenylimino)-acetic acid ethyl ester (4.15)

To a solution of ethyl glyoxalate (50% solution in toluene, 2 mL) in 40 mL dry CH_2Cl_2, a solution of p-anisidine (1.21 g, 9.80 mmol) in 10 mL dry CH_2Cl_2 was added dropwise. The mixture was stirred at r.t. for 30 minutes. Then, molsieves 4 Å (2.5 g) were added, and the mixture was stirred at r.t. overnight. The mixture was filtered over Celite®, and the solvent of the filtrate was evaporated. 1.87 g (92 %) of a brownish oil was obtained which was used as such in the next reaction step.

^{1}H NMR (200 MHz, $CDCl_3$) δ 1.35-1.43 (t, 3H, $CH_2\mathit{CH_3}$), 3.82 (s, 3H, OCH_3), 4.35-4.45 (q, 2H, CH_2), 6.90-6.94 (dd, *J*=6.8 Hz, 2H, ArH), 7.33-7.37 (dd, *J*=6.8 Hz, 2H, ArH), 7.93 (s, 1H, CH) ppm; ^{13}C NMR (50 MHz, $CDCl_3$) δ 146.5, 122.1, 113.0, 60.4, 54.0, 12.7 ppm; IR (NaCl) 2981, 1739, 1713, 1588, 1505, 1290, 1251, 1031, 838 cm^{-1}; GCMS m/z 207 (M).

General method for the samarium diiodide catalyzed coupling reaction

(4-Methoxy-phenylamino)-[4-oxo-1-(toluene-4-sulfonyl)-1,2,3,4-tetrahydroquinolin-3-yl]-acetic acid ethyl ester (4.16a)

The solvent of a samarium diiodide solution in THF (0.1 M in THF, 1.6 mL) was removed by placing the flask under vacuum. To the dry yellow solid, kept under an Ar atmosphere, dry CH_2Cl_2 was added. Freshly prepared (4-methoxy-phenylimino)-acetic acid ethyl ester (**4.15**, 0.33 g, 1.59 mmol) in 2 mL CH_2Cl_2 was added, stirring the mixture under Ar at r.t.. Then, the freshly prepared 1-(toluene-4-sulfonyl)-4-trimethylsilanyloxy-1,2-dihydroquinoline (**4.14a**, 1.6 mmol) in 2 mL dry CH_2Cl_2 was added dropwise. The syringe was washed with 1 mL CH_2Cl_2. The resulting brown mixture was stirred at r.t. under Ar overnight. Then, 10 mL 0.1N HCl was added with vigorous stirring to quench the reaction. The layers were separated, and the aqueous layer was extracted with CH_2Cl_2. The combined organic layers were washed with brine, dried ($MgSO_4$), filtered, and the solvent was evaporated. The product, which could be seen as a brightly yellow spot on TLC with I_2 oxidation, was purified by column chromatography (silica, petroleum ether:EtOAc 4:1). A yellow foam was obtained (0.41 g, 50%, mix of diastereomers).
^{1}H NMR (200 MHz, $CDCl_3$) δ 1.06-1.29 (dt, 3H, $CH_2\mathit{CH_3}$), 2.32-2.37 (ds., 3H, Tos-CH_3), 2.92-2.98 (m, 1H), 3.82-3.96 (m, 1H), 3.75-3.78 (ds, OCH_3), 4.06-4.22 (m, 3H), 4.43-4.44 (d, 1H), 4.55-4.67 (m, 1H), 6.56-7.97 (m, 12H, ArH) ppm; ^{13}C NMR (50 MHz, $CDCl_3$) δ 191.5, 169.5, 151.7, 142.9, 140.6, 138.7, 134.9, 133.4, 128.6, 126.3, 125.2, 124.2, 124.1, 123.1, 114.0, 113.4, 60.3, 55.0, 54.2, 46.4, 45.6, 20.0, 12.4 ppm; IR (NaCl) 3372, 2982, 2930, 1735, 1687, 1597, 1513, 1458, 1359, 1295, 1239, 1164, 1088, 1036, 820, 766, 663 cm^{-1}; MS m/z 509 $(M+H)^+$; GCMS m/z 385 (M-(p-MeO-phenylamine)).

(1-Acetyl-4-oxo-1,2,3,4-tetrahydroquinolin-3-yl)-(4-methoxy-phenylamino)-acetic acid ethyl ester (4.16b)

The product was purified by column chromatography (silica, EtOAc:Hex 1:2 → 2:1). The collected pure fractions gave 0.44 g (42 % over two reaction steps) of a yellow foam.
^{1}H NMR (200 MHz, $CDCl_3$) δ 1.06-1.10 (t, 3H, $CH_2\mathit{CH_3}$), 2.33 (s, 3H, $AcCH_3$), 3.45-3.50 (m, 1H, CH), 3.73 (s, 3H, OCH_3), 3.92-3.98 (t, 1H, CH), 4.07-4.14 (m, 2H, $\mathit{CH_2}CH_3$), 4.25-4.30 (q, 1H, CH), 4.43 (s, 1H, CH), 4.68 (bs, 1H, NH), 6.68-6.71 (d, 2H, ArH), 6.77-6.80 (d, 2H, ArH), 7.26-7.30 (m, 1H, ArH), 7.45-7.57 (m, 2H, ArH), 8.02-8.04 (2, 1H, ArH) ppm; ^{13}C NMR (50 MHz, $CDCl_3$) δ 194, 171.6, 169.7, 153.2, 143.7, 140.6, 134.3, 127.8, 126.2, 125.5, 123.9, 115.7, 114.9, 62.0, 57.8, 55.7, 51.0, 45.7, 23.2, 13.8 ppm; IR (NaCl) 3361, 1983, 1737, 1666, 1600, 1514, 1372, 1304, 1238, 1035, 824, 767 cm^{-1}; MS m/z 397 $(M+H)^+$.

[4-Oxo-1-(toluene-4-sulfonyl)-1,4-dihydro-2H-quinolinylidene]-acetic acid ethyl ester (4.17)

Obtained as a major side-product during purification of **4.16a**.
^{1}H NMR (200 MHz, $CDCl_3$) δ 1.40-1.43 (bd, 3H, $CH_2\mathit{CH_3}$), 2.35 (s, 3H, $TosCH_3$), 4.30-4.34 (bd, 2H, $\mathit{CH_2}CH_3$), 5.25 (s, 2H, NCH_2), 6.49 (s, 1H, C=CH), 7.07-7.10 (d, 2H, ArH), 7.24-7.27 (d, 2H, ArH), 7.39-7.43 (d, 2H, ArH), 7.68-7.72 (d, 2H, ArH), 7.81-7.93 (m, 2H, ArH) ppm; ^{13}C NMR (50 MHz, $CDCl_3$) δ 191.9, 180.0, 163.5, 143.2, 141.2, 140.6, 133.4, 132.6, 128.2, 126.7, 126.3, 126.0, 125.7, 123.2, 59.8, 46.0, 20.1, 12.7 ppm; IR (KBr) 2933, 1714, 1683, 1597, 1459, 1361, 1299, 1250, 1165, 1061, 680 cm^{-1}; GCMS m/z 385 (M); MS m/z 386 $(M+H)^+$, 403 $(M+NH_4)^+$, 424 $(M+K)^+$.

Amino-[4-oxo-1-(toluene-4-sulfonyl)-1,2,3,4-tetrahydroquinolin-3-yl]-acetic acid ethyl ester (4.18)

A solution of (4-methoxy-phenylamino)-[4-oxo-1-(toluene-4-sulfonyl)-1,2,3,4-tetrahydroquinolin-3-yl]-acetic acid ethyl ester (**4.16a**, 0.34g, 0.66 mmol) in acetonitrile (50 mL) was cooled on an ice/water bath. A solution of ceric ammonium nitrate (1.09g, 1.98 mmol) in water (10 mL) was added dropwise, turning the color of the solution from yellow to blue/black to brown/black to orange over several minutes. The reaction was left to warm to r.t. and stirred at r.t. for 1 hour. The mixture was concentrated in vacuo. Water was added, and the aqueous layer was extracted with EtOAc. The combined organic layers were washed with brine, dried ($MgSO_4$), filtered, and the solvent was evaporated. The product was purified by column chromatography (silica, petroleum ehter: EtOAc 1:1 to pure EtOAc). A brown oil was obtained which was not pure enough for full characterization. ^{13}C NMR (50 MHz, $CDCl_3$) δ 192.0, 189.2, 143.1, 140.8, 134.6, 133.9, 133.5, 128.7, 126.9, 126.0, 125.9, 123.6, 123.04 ppm; IR (NaCl) 3393, 3331, 2980, 2927, 1735, 1688, 1597, 1458, 1358, 1165, 1088, 766, 733, 674 cm^{-1}; MS m/z 403 $(M+H)^+$, 386 $(M-NH_3+H)^+$.

Acetylamino-(1-acetyl-4-oxo-1,2,3,4-tetrahydroquinolin-3-yl)-acetic acid ethyl ester (4.25)

To a solution of iodobenzene diacetate (2.00 g, 6.20 mmol) in methanol (50 mL), a solution of (1-acetyl-4-oxo-1,2,3,4-tetrahydroquinolin-3-yl)-(4-methoxy-phenylamino)-acetic acid ethyl ester (**4.16b**, 0.61 g, 1.55 mmol) in methanol (15 mL) was added dropwise over 20 minutes. The mixture was stirred at r.t. for 1.5 hours. 1 N HCl (50 mL) was added, and the mixture was stirred for 0.5 h at r.t.. Then, the mixture was washed with CH_2Cl_2 (2x). The combined organic layers were back-extracted with 0.1 N HCl (1x30 mL). Then, CH_2Cl_2 (50 mL) was added to the combined aqueous layers, followed by acetic anhydride (0.72 mL, 0.79 g, 7.7 mmol). The mixture was brought to pH 8-9 by addition of solid K_2CO_3, turning the color of the mixture to purple/brown. The biphasic mixture was stirred at room temperature for 1.5 h. The layers were then separated, and the aqueous phase was extracted with CH_2Cl_2. The combined organic layers were washed with brine, dried ($MgSO_4$), filtered, and the solvent was evaporated. The product was purified by column chromatography (silica, CH_2Cl_2:MeOH 100:1→ 50:1), yielding 126 mg (25 %) of an off-white solid.

^1H NMR (200 MHz, $CDCl_3$) δ 1.20-1.27 (t, 3H, $CH_2\mathit{CH_3}$), 1.99 (s, 3H, $COCH_3$), 2.37 (s, 3H, $COCH_3$), 3.60-3.67 (m, 2H, NCH_2), 4.17-4.28 (q, 2H, $\mathit{CH_2}CH_3$), 4.76-4.81 (d, *J*=9.97, 1H, CH), 4.94-4.99 (dd, 1H, CH), 6.28-6.32 (d, *J*=8.22, 1H, NH), 7.20-7.28 (m, 1H, ArH), 7.54-7.56 (d, *J*=3.81, 1H, ArH), 7.94-7.98 (d, *J*=7.92, 1H, ArH) ppm; ^{13}C NMR (50 MHz, $CDCl_3$) δ 194.2, 170.7, 170.2, 169.6, 144.0, 134.7, 127.7, 125.4, 125.1, 124.2, 62.2, 51.6, 50.5, 47.6, 23.5, 23.1, 14.0 ppm; IR (KBr) 3295, 2951, 1742, 1673, 1536, 1478, 1371, 1245, 1216, 766 cm^{-1}.

(1-Acetyl-4-oxo-1,2,3,4-tetrahydroquinolin-3-yl)-tert-butoxycarbonylamino-acetic acid ethyl ester (4.26)

To a solution of iodobenzene diacetate (1.75g, 5.44 mmol) in methanol (20 mL), (1-acetyl-4-oxo-1,2,3,4-tetrahydroquinolin-3-yl)-(4-methoxy-phenylamino)-acetic acid ethyl ester (**4.16b**, 0.54 g, 1.4 mmol) in 15 mL methanol was added dropwise over 20 min. The reaction was stirred for 1 h at r.t., and was then acidified with 1 N HCl (35 mL). After stirring for 1.5 h at r.t., the mixture was concentrated in vacuo. The remaining aqueous layer was washed with CH_2Cl_2 (2x). The combined organic layers were back-extracted with 30 mL 0.1 N HCl. The combined aqueous layers were stirred with CH_2Cl_2 (30 mL), and Boc_2O (0.44 g, 2.0 mmol) was added with some CH_2Cl_2, followed by K_2CO_3 to pH 8-9. The mixture was stirred vigorously at r.t. for 2.3 h. The layers were separated, and the aqueous layer was extracted with CH_2Cl_2. The combined organic layers were washed with brine, dried ($MgSO_4$), filtered, and the solvent was evaporated. The product was purified

with column chromatography (silica, hexane:EtOAc 4:1→1:1). The product was isolated as an oil (147 mg, 28 %).
^{1}H NMR (200 MHz, $CDCl_3$) δ 1.15-1.26 (q, 3H, CH_2CH_3), 1.39-1.41 (d, 9H, BOC-CH_3), 2.35-2.36 (d, 3H, $COCH_3$), 3.63-3.67 (d, *J*=7.92 Hz, 2H, CH_2), 4.13-4.23 (m, 2H, CH_2CH_3), 4.57-4.82 (dd, 1H, CH), 4.70-4.82 (m, 1H, CH), 5.23-5.28 (d, *J*=8.22, 1H, CH), 7.19-7.27 (m, 1H, ArH), 7.52-7.54 (d, *J*=4.7 Hz, ArH), 7.94-7.99 (dd, 1H, ArH) ppm; ^{13}C NMR (50 MHz, $CDCl_3$) δ 194.0, 170.56, 169.6, 156.0, 143.9, 134.5, 127.8, 125.4, 124.1, 80.3, 62.0, 52.4, 51.5, 47.3, 28.2, 23.4, 14.0 ppm; IR (NaCl) 3346, 1979, 1729, 1674, 1600, 1480, 1371, 1245, 1163, 1029, 958, 860, 768 cm^{-1}; MS (ESI) m/z 391 $(M+H)^+$, 408 $(M+NH_4)^+$, 413 $(M+Na)^+$.

4-Oxo-3,4-dihydro-2H-quinoline-1-carboxylic acid tert-butyl ester (4.27)
A solution of **4.4** (1.01 g, 6.89 mmol), di-tert-butyl dicarbonate (1.82 g, 8.34 mmol), and N,N-dimethylaminopyridine, (DMAP, 1.01 g, 8.27 mmol) in THF (25 mL) was stirred at r.t.. After 4 h, no starting material was left by TLC. Water was added, and EtOAc. The organic layer was washed with water (3x). The combined aqueous layers were back-extracted with EtOAc (2x). The combined organic layers were washed with brine (1x), dried ($MgSO_4$), filtered, and the solvent was evaporated. The crude product was purified by column chromatography (silica, Hex/EtOAc) as a white solid (1.15 g, 68%).
^{1}H NMR (200 MHz, $CDCl_3$) δ 1.55 (s, 9H, $C(CH_3)_3$), 2.73-2.80 (t, 2H, CH_2), 4.12-4.18 (t, 2H, CH_2), 7.11-7.19 (m, 1H, ArH), 7.44-7.53 (m, 1H, ArH), 7.74-7.78 (d, *J*=8.43Hz, 1H, ArH), 7.96-8.00 (dd, *J*=1.46, 7.69Hz, 1H, ArH) ppm; ^{13}C NMR (50 MHz, $CDCl_3$) δ 133.9, 127.3, 123.9, 123.7, 82.2, 44.3, 39.0, 28.3 ppm; GCMS m/z 247 (M); IR (KBr) 2982, 1686, 1600, 1476, 1359, 1153, 766 cm^{-1}.

4-Trimethylsilanyloxy-2H-quinoline-1-carboxylic acid tert-butyl ester (4.28)
Synthesized according to general procedure.
IR (NaCl) 2973, 1712, 1694, 1486, 1370, 1345, 1250, 1223, 1152, 881, 846, 757 cm^{-1}.

3-[Ethoxycarbonyl-(4-methoxy-phenylamino)-methyl]-4-oxo-3,4-dihydro-2H-quinoline-1-carboxylic acid tert-butylester (4.29)
Synthesized according to general procedure. The product was purified by column chromatography (silica, Hex:EtOAc 10:1 → 5:1). The product was isolated in 3 fractions. The first fraction contained diastereomer 1 (upper spot on TLC, 2.94 g), the second fraction contained both diastereomers (0.85 g, and the third fraction contained diastereomer 2 (lower spot on TLC, 0.67 g). In total, 4.46 g product was yielded (40% over two steps).
First fraction:
^{1}H NMR (300 MHz, $CDCl_3$) δ 0.97-1.01 (t, 3H, $COOCH_2CH_3$), 1.57 (s, 9H, BOC-CH_3), 3.42-3.44 (m, 1H, $(C=O)CH_2$), 3.74 (s, 3H, $ArOCH_3$), 4.02-4.16 (m, 3H, NCH_2 and OCH_2CH_3), 4.29-4.35 (dd, *J*=4.76, 13.55 Hz, 1H, NCH_2), 4.41-4.42 (d, *J*=3.67 Hz, 1H, NH*CH*), 6.68-6.71 (m, 2H, ArH), 6.77-6.81 (m, 2H, ArH), 7.13-7.17 (t, 1H, ArH), 7.46-7.51 (dt, 1H, ArH), 7.74-7.76 (d, *J*=8.43 Hz, ArH), 7.99-8.02 (dd, *J*=1.47, 7.69 Hz, 1H, ArH) ppm; ^{13}C NMR (50 MHz, $CDCl_3$) δ 194.4, 171.8, 153.3, 152.9, 144.1, 140.7, 134.3, 127.6, 125.3, 124.0, 123.5, 115.7, 115.2, 82.8, 62.0, 57.5, 56.0, 50.2, 45.8, 28.5, 13.8 ppm; IR (NaCl) 3384, 2980, 2935, 1739, 1713, 1693, 1681, 1514, 1369,m 1235, 1151, 1035, 821, 765 cm^{-1}; HRMS m/z obs. 455.21810, calc. 455.21766 $(M+H)^+$.
Second fraction:
^{1}H NMR (300 MHz, $CDCl_3$) δ 1.18-1.23 (t, 3H, $COOCH_2CH_3$), 1.52 (s, 9H, BOC-CH_3), 3.13-3.19 (m, 1H, (C=O)CH), 3.73 (3H, $ArOCH_3$), 4.02-4.22 (dd and m, 3H, NCH_2 and $COOCH_2CH_3$), 4.43-4.52 (dd and d, 2H, NCH_2 and NCH), 6.76 (s, *ArH*-OMe), 7.12-7.17 (t, 1H, ArH), 7.47-7.53 (dt, 1H, ArH), 7.76-7.79 (d, *J*=8.05 Hz, 1H, ArH), 7.97-8.00 (dd, 1H, ArH) ppm; ^{13}C NMR (50 MHz, $CDCl_3$) δ 194.1, 172.8, 153.7, 152.9, 144.2, 141.0, 134.4, 127.9, 125.0, 124.2, 123.8, 116.8, 115.0, 82.6, 77.9, 77.2, 76.6, 61.9, 58.2, 55.9, 50.7,

46.3, 28.4, 14.4 ppm; IR (KBr) 3359, 2976, 1735, 1700, 1683, 1516, 1387, 1262, 1238, 1159, 1036, 827, 758 cm^{-1}; HRMS m/z obs. 455.21799, calc. 455.21766 $(M+H)^+$.

3-[1-Ethoxycarbonyl-methylidene]-4-oxo-3,4-dihydro-2H-quinoline-1-carboxylic acid *tert*-butyl ester (4.30)

Isolated as a side-product during the synthesis of **4.29**.
^{1}H NMR (200 MHz, $CDCl_3$) δ 1.304-1.376 (t, 3H, $OCH_2\mathit{CH_3}$), 1.53 (s, 9H, $OC(CH_3)_3$), 4.23-4.33 (q, *J*=7.05, 14.39 Hz, 2H, $O\mathit{CH_2}CH_3$), 5.30 (s, 2H, NCH_2), 6.88 (s, 1H, C=CH), 7.17-7.24 (t, *J*=7.35, 7.64 Hz, 1H, ArH), 7.50-7.58 (t, *J*=7.35, 8.22 Hz, 1H, ArH), 7.69-7.73 (2, *J*=8.22 Hz, 1H, ArH), 7.96-8.00 (d, *J*=7.64Hz, 1H, ArH) ppm; ^{13}C NMR (50 MHz, $CDCl_3$) δ 183.6, 165.4, 152.8, 144.8, 144.2, 134.6, 128.4, 126.2, 124.9, 124.6, 123.9, 82.6, 61.4, 46.0, 28.4, 14.4 ppm; IR (NaCl) 2977, 1721, 1713, 1680, 1601, 1479, 1154, 758 cm^{-1}; MS m/z 332 $(M+H)^+$, 349 $(M+NH_4)^+$, 354 $(M+Na)^+$.

3-(*tert*-Butoxycarbonylamino-ethoxycarbonyl-methyl)-4-oxo-3,4-dihydro-2*H*-quinoline-1-carboxylic acid *tert*-butyl ester (4.31)

Prepared as described for compound **4.26** from diastereomer 1(upper) of **4.29**. A mixture of diastereomers was obtained (0.87 g, 30 %) by column chromatography (silica, Hex: EtOAc 10:1 → 5:1). Diastereomers could be separated by column chromatography (silica, Hex: EtOAc (10:1 → 15:2) in a final total yield of 15 %.
First fraction:
^{1}H NMR (400 MHz, $CDCl_3$) δ 1.20-1.24 (t, 3H, *J*=6.97 Hz, $OCH_2\mathit{CH_3}$), 1.41 (s, 8H (expect 9H), BOC-CH_3), 1.56 (s, 8H (expect 9H), BOC-CH_3), 3.63-3.73 (m, 2H, (C=O)CH and NCH_2), 4.20-4.23 (m, 2H, $O\mathit{CH_2}CH_3$), 4.57-4.71 (m, 2H, NCH_2 and NH), 5.24-5.26 (d, *J*=8.79 Hz, 1H, NHCH), 7.11-7.15 (t, 1H, ArH), 7.47-7.51 (m, 1H, ArH), 7.77-7.79 (d, *J*=8.43 Hz, 1H, ArH), 7.93-7.95 (dd, 1H, ArH) ppm; ^{13}C NMR (50 MHz, $CDCl_3$) δ 194.5, 170.92, 156.29, 152.9, 144.5, 134.6, 127.6, 124.5, 124.0, 123.8, 82.8, 80.5, 62.2, 52.5, 50.7, 47.3, 28.5, 28.5, 14.2 ppm; IR (NaCl) 3347, 2978, 2933, 1738-1682, 1602, 1479, 1368, 1325, 1247, 1220, 1157, 1071, 1029, 858, 765, 736 cm^{-1}; MS m/z 449 $(M+H)^+$, 466 $(M+NH_4)^+$, 471 $(M+Na)^+$, 897 $(2M+H)^+$, 914 $(2M+NH_4)^+$, 919 $(2M+Na)^+$.
Second fraction:
^{1}H NMR (400 MHz, $CDCl_3$) δ 1.19-1.23 (t, 3H, $OCH_2\mathit{CH_3}$), 1.43 (s, 9H, BOC-CH_3), 1.56 (s, 8H (expected 9H), BOC-CH_3), 3.13-3.18 (m, 1H, (C=O)CH), 4.00-4.06 (bt, 1H, NCH_2), 4.13-4.20 (m, 2H, $O\mathit{CH_2}CH_3$), 4.57-4.58 (m, 2H, NCH_2 and NH), 5.64-5366 (bd, *J*=8.43Hz, NHCH), 7.11-7.15 (t, 1H, ArH), 7.47-7.51 (m, 1H, ArH), 7.78-7.80 (d, *J*=8.07Hz, 1H, ArH), 7.94-7.96 (dd, 1H, ArH) ppm; ^{13}C NMR (50 MHz, $CDCl_3$) δ 195.1, 170.9, 155.6, 152.8, 144.4, 134.6, 127.7, 124.6, 124.1, 123.7, 82.8, 80.4, 62.0, 53.2, 51.3, 47.6, 28.5, 14.3 ppm; IR NaCl 3362, 2980, 2933, 1745-1680, 1601, 1480, 1370, 1299, 1221, 1152, 858, 767, 732 cm^{-1}; MS m/z 449 $(M+H)^+$, 466 $(M+NH_4)^+$, 471 $(M+Na)^+$, 897 $(2M+H)^+$, 914 $(2M+NH_4)^+$, 919 $(2M+Na)^+$.

3-(*tert*-Butoxycarbonylamino-carboxymethyl)-4-oxo-3,4,-dihydro-2*H*-quinoline-1-carboxylic acid *tert*-butyl ester (4.32)

A mixture of 3-(t*ert*-butoxycarbonylamino-ethoxycarbonyl-methyl)-4-oxo-3,4-dihydro-2*H*-quinoline-1-carboxylic acid tert-butyl ester (**4.31**, 0.440 g, 0.980 mmol), 5 mL EtOH, 5 mL H_2O and KOH (0.102 g, 1.81 mmol) was stirred at room temperature. After 4 hours, NH_4Cl (sat. aq.) was added and some 1 N HCl for acidification. The aqueous layer was extracted with EtOAc. The combined organic layers were washed with brine, dried ($MgSO_4$), filtered, and the solvent was evaporated, yielding 0.433 g of a colorless oil/white foam (quant. yield). TLC and HPLC analysis showed the presence of both diastereomers.
^{1}H NMR (400 MHz, $CDCl_3$) δ [1.40; 1.43] (2 x s, 9H, BOC-CH_3), [1.55; 1.56] (2 x s, 9H, BOC-CH_3), [3.19-3.22; 3.6-3.73; 3.95-4.01] ([m, m, bt], 2H, [(C=O)CH diastereomer 1; (C=O)CH and NCH_2 diastereomer 2; NCH_2 diastereomer 1]), 4.63-4.76 (m, 2H, NCH_2 and NH; on bs of COOH); 5.27-5.30 and 5.80-5.82 (d and bd, 1H, NHCH) ppm; ^{13}C NMR (50 MHz, $CDCl_3$) δ 194.7, [175.3, 174.4], 156.3, [153.0, 152.9], 144.6, 134.8, [127.9, 127.7],

[124.4, 124.3], [124.2, 124.1], [123.9, 123.8], [83.0, 80.8], 52.0, [51.0, 50.7], 47.5, 28.52, 28.48, 28.45 ppm; IR (KBr) 3382, 2976, 1715, 1686, 1601, 1479, 1368, 1156, 856, 766 cm^{-1}.

Amino-(4-oxo-1,2,3,4-tetrahydroquinolin-3-yl)-acetic acid (4.2)
A mixture of 3-(*tert*-butoxycarbonylamino-carboxymethyl)-4-oxo-3,4,-dihydro-2*H*-quinoline-1-carboxylic acid *tert*-butyl ester (**4.32**, 0.506 g, 1.20 mmol), CH_2Cl_2 (10 mL), and trifluoroacetic acid (2 mL) was stirred at room temperature. After 3.5 hours, 1 mL of trifluoroacetic acid was added and the mixture was stirred for 0.5 hours. The solvent and trifluoroacetic acid were evaporated. The product was purified by column chromatography (silica, CH_2Cl_2 → CH_2Cl_2/MeOH 10:1 → MeOH), yielding 0.146 g of a yellow solid. This fraction was triturated with acetone/MeOH to yield 0.142 g of the pure product as a brightly yellow solid (53 %).
^{1}H NMR (500 MHz, D_2O) δ 3.26-3.31 (m, 1H, NH_2*CH*), [3.35-3.40, 3.46-3.48, 3.54-3.59] ([dt, m, dd], 2H, [(C=O)CH of diastereomer 1, (C=O)CH and NCH_2 of diastereomer 2, NCH_2 of diastereomer 1]), 4.21-4.23 (m, 1H, NCH_2), 6.57-6.71 (dd (*J*=8.3 Hz) and dt, 2H, ArH), 7.15-7.22 (dt, 1H, ArH), 7.41-7.47 (dd, *J*= 7.81, 21.24 Hz, 1H, ArH) ppm; ^{13}C NMR (125 MHz, D_2O) δ [194.0, 193.2], [170.2, 170.1], [150.6, 149.3], 137.13, 137.07], [127.49, 127.46], [121.1, 120.1], [119.2, 118.6], [118.2, 117.6], [51.0, 50.9], [46.1, 45.7], [44.0, 43.2] ppm; IR (KBr) 3379, 2952, 1668, 1644, 1618, 1492, 1405, 1246, 1151, 745
cm^{-1}; HRMS $(M+H)^+$ m/z obs. 221.09212 calc. 21.09207 ($C_{11}H_{13}O_3N_2$).

3-Carboxymethyl-4-oxo-3,4-dihydro-2*H*-quinoline-1-carboxylic acid tert-butyl ester (4.34)
A solution of 4-oxo-3,4-dihydro-2*H*-quinoline-1-carboxylic acid tert-butyl ester (**4.27**, 0.853 g, 3.45 mmol) in 20 mL THF under N_2 was cooled to -80 °C. A solution of LHMDS (0.891 g, 5.32 mmol) in 5 mL THF was added dropwise, changing the color from yellow to dark yellow. The mixture was left to warm up to -15 °C over 1 h. Then, it was cooled back to -80 °C and ethyl bromoacetate (0.38 mL, 0.58 g, 3.45 mmol) was added at once. The reaction mixture was left to warm up to r.t.. After 3.75 h the reaction was quenched by addition of water. The layers were separated and the aqueous layer was extracted with EtOAc. The combined organic layers were dried ($MgSO_4$), filtered, and the solvent was evaporated. The product was partially purified by column chromatography (silica, Hex:EtOAc), yielding 0.698 g of an oil which contained **4.33** as the main component.
IR (NaCl) 2980, 1736-1686, 1601, 1476, 1363, 1234, 1156, 765 cm^{-1}.
The product was stirred at r.t. in 10 mL EtOH and 10 mL 1 N NaOH for 1 h. More water was added. Washing with CH_2Cl_2 gave an emulsion. The mixture was acidified with saturated NH_4Cl and some 1 N HCl and was extracted with CH_2Cl_2. The combined organic layers were extacted with saturated $NaHCO_3$ solution. The combined aqueous extracts were acidified with 1 N HCl and extracted with CH_2Cl_2. The combined organic extracts were dried ($MgSO_4$), filtered, and the solvent was evaporated. Column chromatography (silica, CH_2Cl_2) gave the pure product as a colorless oil, which solidified over time to obtain a white solid (0.343 g, 33 % overall yield).
^{1}H NMR (200 MHz, $CDCl_3$) δ 1.55 (s, 9H, BOC-$(CH_3)_3$),2.51-2.64 (q, 1H, *CH*$_2$COOH), 2.88-2.99 (dd, *J*=4.70, 17.34Hz, 1H, *CH*$_2$COOH), 3.11-3.25 (m, 1H, CH), 3.68-3.80 (q, *J*=11, 13.22 Hz, CH_2), 4.51-4.60 (q, *J*=4.40, 13.22 Hz, CH_2), 7.12-7.19 (t, 1H, ArH), 7.47-7.55 (dt, 1H, ArH), 7.78-7.82 (d, *J*= 8.52 Hz, 1H, ArH), 7.97-8.01 (dd, *J*=1.18, 7.94 Hz, 1H, ArH), 9.32 (bs, 1H, COOH) ppm; ^{13}C NMR (50 MHz, $CDCl_3$) δ 195.1, 177.1, 153.0, 144.4, 134.5, 127.9, 124.3, 124.2, 123.8, 82.7, 48.5, 44.3, 32.1, 28.4 ppm; IR (KBr) 3048, 2975, 1709, 1702, 1689, 1599, 1482, 1368, 1156, 764 cm^{-1}.

(4-Oxo-1,2,3,4-tetrahydroquinolin-3-yl)-acetic acid (4.3)
A mixture of 3-carboxymethyl-4-oxo-3,4-dihydro-2*H*-quinoline-1-carboxylic acid tert-butyl ester (**4.34**, 0.198 g, 0.648 mmol) and TFA (0.050 mL) in 10 mL CH_2Cl_2 was stirred at r.t..

The reaction mixture was stirred over two days, and a total of 0.3 mL TFA was added in portions. The solvent was evaporated. The crude product was subjected directly to column chromatography (silica, CH_2Cl_2: MeOH 25:1). The pure product was obtained as a brightly yellow solid (75.4 mg, 57 %).
^{1}H NMR (200 MHz, CD_3OD) δ 2.22-2.34 (dd, 1H, *CH*$_2$COOH), 2.66-2.77 (dd, *J*=5.29, 16.75 Hz, 1H, *CH*$_2$COOH), 2.83-2.99 (m, 1H, CO*CH*), 3.15-3.27 (m + solvent residual peak of CD_3OD, 1H, NH*CH*$_2$), 3.43-3.52 (dd, *J*=5.59, 11.75 Hz, 1H, NH*CH*$_2$), 6.49-6.59 (ddd, *J*=0.88, 7.93 Hz, 1H, ArH), 6.62-6.66 (d, *J*=8.52 Hz, 1H, ArH), 7.13-7.21, (ddd, *J*=1.47, 7.05 Hz, 1H, ArH), 7.56-7.61 (dd, *J*=1.47, 7.94 Hz, 1H, ArH) ppm; ^{13}C NMR (50 MHz, $CDCl_3$) δ 195.6, 174.5, 153.3, 135.2, 127.1, 117.7, 116.8, 115.9, 45.9, 43.0, 31.5 ppm; IR (KBr) 3367, 2920, 1689, 1654, 1616, 1517, 1240, 747 cm^{-1}; HRMS $(M+H)^+$ m/z obs. 206.08124 calc 21.08117 ($C_{11}H_{12}O_3N_1$).

Kynurenine aminotransferase activity in rat brain homogenate
KAT inhibitory activity was determined in rat brain tissue homogenate as described previously, with modifications.[33, 34] Rat brain (male Wistar rats, whole brain) was homogenized in a 5 mM Tris-acetate buffer at pH 8.0, containing 50 µM pyridoxal 5'-phosphate and 10 mM 2-mercaptoethanol (10 % w/v). The homogenate was dialyzed against this buffer for 24 hours at 4 °C (12 mL homogenate / 2.5 L buffer). Enzyme activity was tested in an assay consisting of 200 µL of dialyzed tissue homogenate, 150 mM Tris acetate buffer, pH 8.0, 70 µM pyridoxal 5'-phosphate, 1 mM pyruvate, 10 µM *L*-kynurenine and the inhibitor in a final volume of 250 µL (all concentrations final). The mixture was incubated at 37 °C for 2 h. The reaction was terminated by addition of 100 µL 7% perchloric acid. The mixture was centrifuged for 15 minutes at 14000 rpm, 4 °C. Kynurenic acid concentrations were determined in the supernatant by HPLC (Supelcosil™ HPLC column, 15 cm x 3 mm, 3 µm). The mobile phase consisted of a buffer containing 15 % methanol, 10 g/L $Na_2HPO_4.2H_2O$, 150 mg/L EDTA and 0.17 % (v/v) THF, adjusted to pH 5.27 with phosphoric acid. The product was detected fluorimetrically at an extinction of 344 nm and emission of 398 nm. Each concentration of inhibitor was assayed in triplo. The KYNA concentration in each sample was determined in triplo.

Kynureninase activity in liver tissue homogenate
Kynureninase activity was determined in rat liver tissue homogenate as described previously, with modifications.[35, 36] Liver tissue was homogenated in a buffer (10% w/v) consisting of 20 mM Tris-acetate pH 8.0, 0.5 mM 2-mercaptoethanol, and 50 µM pyridoxal 5'-phosphate. The homogenate was centrifuged at 14000 rpm for 30 minutes at 4 °C. The supernatant was dialyzed against the buffer as described above (12 mL supernatant / 2.5 L buffer) for 24 hours at 4 °C. Enzyme activity was determined using 100 µL of the dialyzed tissue, 50 µL of a solution consisting of 400 mM Tris-HCl buffer pH 8.0, 200 µM pyridoxal 5'-phosphate and 40 µM *L*-kynurenine (final concentration 10 µM), and 50 µL inhibitor at varying concentrations. The mixture was incubated at 37 °C for 30 minutes. The reaction was terminated by mixing with 100 µL 7% perchloric acid. The samples were centrifuged at 14000 rpm for 15 minutes at 4 °C. Anthranilic acid concentrations in the supernatant were measured by HPLC.
The supernatant was applied to a Supelcosil™ HPLC column (15 cm, 4.6 or 3 mm ID, 3 µm particle size). The mobile phase consisted of a buffer containing 26% methanol, 10 g/L $Na_2HPO_4.2H_2O$, 150 mg/L EDTA and 0.17 % (v/v) THF, adjusted to pH 5.27 with phosphoric acid. The product was detected fluorimetrically at an extinction of 313 nm and emission of 420 nm. Each concentration of inhibitor was assayed in triplo. The anthranilic acid concentration in each sample was determined in triplo.

Kynurenine 3-hydroxylase activity in liver tissue homogenate
Kynurenine 3-hydroxylase activity was determined in rat liver tissue homogenate as described previously, with modifications.[35] The tissue was homogenized in icecold 0.32 M sucrose solution (1 g tissue / 8 mL sucrose solution). The homogenate was centrifuged at

11000 rpm, 4 °C, 30 min. The supternatant was taken off, and the residue was resuspended in sucrose solution (1 mL 0.32 M sucrose / residue of 1 mL homogenate). The tissue was centrifuged (11000 rpm, 4 °C, 30 min). This washing procedure was repeated twice. The resulting tissue was resuspended in 0.14 M KCl, 20 mM potassium phosphate buffer at ph 7.0.
Enzyme activity was measured using 75 µL of the tissue homogenate, 100 µL of a 100 mM potassium phosphate buffer pH 7.5, containing 1 mM NADPH, 4 mM $MgCl_2$, and 20 µM L-kynurenine (final concentration 10 µM), and 25 µL of a solution of the inhibitor at varying concentrations. The mixture was incubated at 37 °C for 30 minutes. The reaction was terminated by the addition of 100 µL 7% perchloric acid. The samples were centrifuged (14000 rpm, 15 minutes, 4°C). The concentrations of 3-hydroxykynurenine in the supernatant were determined by HPLC. The supernatant was applied to a Supelcosil™ HPLC column (15 cm, 4.6 or 3 mm ID, 3 µm particle size). The mobile phase consisted of a solution of 100 mg EDTA, 150 mg heptane sulphonic acid, 5.9 mL phosphoric acid, 9.0 mL triethylamine and 20 mL acetonitrile in 950 mL H_2O.[37] Each concentration of inhibitor was assayed in triplo. The 3-hydroxykynurenine concentration in each sample was determined in triplo.

Molecular Modeling
Hardware and software specifications All computations were preformed on an Intel® Pentium® 4.0 3.0GHz computer with 2 Gb memory, running Ubuntu 8.10 (Intrepid Ibex) as the operating system. For preparation of the macromolecule, ligands, structure minimizations and analysis of ligand-protein interactions Sybyl 8.1 was used.[38] For docking, structures were processed in AutoDockTools (ADT) version 1.5.4.[39] For docking, AutoDock Vina[40] version 1.0.2 was used and results were analyzed in PyMOL version 1.1beta3 (www.pymol.org) as distributed for Ubuntu.
Conformational Search Ligands were built in Sybyl. Conformational searches were preformed for *L*-KYN, **4.2** and **4.3** using the Random search function in Sybyl. For minimization, the Powell method was used with a maximum of 1000 iterations, no Simplex iterations were done. The search was terminated at a gradient of 0.05. Energies were calculated using the Tripos Force Field and Gasteiger-Hückel charges. The Random search was terminated at a maximum of 1000 cycles or a maximum of 50 hits per accepted conformation. The energy cutoff was set at 10 kcal/mol with an RMS threshold of 0.2 Å. All other parameters were kept at the default values. The bicyclic quinolinone core was built as a planar structure to unbias the search. All except the aromatic bonds were activated for the search.
From each search, the conformation with the lowest energy was regarded as the global minimum. These conformations were inspected on the orientation of the aliphatic branch of the molecule. The global minima with the branch in an equatorial orientation were selected for docking. If the branch was oriented axially, the conformation with an equatorial orientation at the lowest possible energy was selected for docking.
All molecules selected for docking were aligned by the Database align function in Sybyl, using the aromatic ring and the carboxylic acid functions as template groups.
Docking For docking, the crystal structure of human KYNase in complex with 3-hydroxyhippuric acid (PDB ID 3E9K[28], www.rcsb.org) was used as the enzyme structure. From this structure, the ligand was extracted. The biological dimeric unit was created in PyMOL. The dimeric enzyme structure without the ligand was loaded into AutoDockTools and prepared as the macromolecule. Only polar hydrogen atoms were taken into account. The small molecule structures were loaded into AutoDockTools and prepared as the ligand structure. The Grid box dimensions were determined from the co-crystallized ligand 3-hydroxyhippuric acid according to the method as used for AutoDock Vina evaluation.[40] In summary, the smallest possible box was created around the co-crystallized ligand. Along each axis, this box was extended by 10 Å. For each axis, the box was extended by another 5 Å in one of the two directions, (semi)-randomly chosen. If the resulting size of the box in either direction was less than 22.5 Å, the size was adjusted to this minimum value. This

resulted in a box with center coordinates (x,y,z)=(1.959, 2.830, 13.629) and dimensions in Å of (x,y,z) = (23, 22.5, 23). This box was used for all docking experiments. The exhaustiveness parameter was set to a value of 15. All other parameters were kept at their default values. The results were analyzed in PyMOL. Conformations were compared to the conformation of 3-hydroxyhippuric acid. In addition, conformations of **4.2**, **4.3** and **4.36** were compared to the conformation of docked *L*-KYN. Unless stated otherwise, the conformation with the lowest possible energy was regarded as the best docked hit.
Analysis of interactions The best docked conformations for each ligand were merged into the macromolecule structure in Sybyl. Static hydrogen bonds were added, using standard settings of Sybyl.
Figures Figures 1-7 were generated in PyMOL (www.pymol.org).

4.7 References

1. Perkins, M. N.; Stone, T. W. An iontophoretic investigation of the actions of convulsant kynurenines and their interaction with the endogenous excitant quinolinic acid. *Brain Res.* **1982,** 247, 184-187.
2. Parsons, C. G.; Danysz, W.; Quack, G.; Hartmann, S.; Lorenz, B.; Wollenburg, C.; Baran, L.; Przegalinski, E.; Kostowski, W.; Krzascik, P.; Chizh, B.; Max. Headley, P. Novel Systemically Active Antagonists of the Glycine Site of the N-Methyl-D-aspartate Receptor: Electrophysiological, Biochemical and Behavioral Characterization. *J. Pharmacol. Exp. Ther.* **1997,** 283, 1264-1275.
3. Hilmas, C.; Pereira, E. F.; Alkondon, M.; Rassoulpour, A.; Schwarcz, R.; Albuquerque, E. X. The brain metabolite kynurenic acid inhibits alpha7 nicotinic receptor activity and increases non-alpha7 nicotinic receptor expression: physiopathological implications. *J. Neurosci.* **2001,** 21, 7463-7473.
4. Stone, T. W. Neuropharmacology of quinolinic and kynurenic acids. *Pharmacol. Rev.* **1993,** 45, 309-379.
5. Wang, J.; Simonavicius, N.; Wu, X.; Swaminath, G.; Reagan, J.; Tian, H.; Ling, L. Kynurenic acid as a ligand for orphan G protein-coupled receptor GPR35. *J. Biol. Chem.* **2006,** 281, 22021-22028.
6. Pearson, S. J.; Reynolds, G. P. Increased brain concentrations of a neurotoxin, 3-hydroxykynurenine, in Huntington's disease. *Neurosci. Lett.* **1992,** 144, 199-201.
7. Guidetti, P.; Luthi-Carter, R. E.; Augood, S. J.; Schwarcz, R. Neostriatal and cortical quinolinate levels are increased in early grade Huntington's disease. *Neurobiol. Dis.* **2004,** 17, 455-461.
8. Reynolds, G. P.; Pearson, S. J.; Halket, J.; Sandier, M. Brain Quinolinic Acid in Huntington's Disease. *J. Neurochem.* **1988,** 50, 1959-1968.
9. Schwarcz, R.; Rassoulpour, A.; Wu, H. Q.; Medoff, D.; Tamminga, C. A.; Roberts, R. C. Increased cortical kynurenate content in schizophrenia. *Biol. Psychiatry* **2001,** 50, 521-530.
10. Erhardt, S.; Blennow, K.; Nordin, C.; Skogh, E.; Lindstrom, L. H.; Engberg, G. Kynurenic acid levels are elevated in the cerebrospinal fluid of patients with schizophrenia. *Neurosci. Lett.* **2001,** 313, 96-98.
11. Nilsson, L. K.; Linderholm, K. R.; Engberg, G.; Paulson, L.; Blennow, K.; Lindstrom, L. H.; Nordin, C.; Karanti, A.; Persson, P.; Erhardt, S. Elevated levels of kynurenic acid in the cerebrospinal fluid of male patients with schizophrenia. *Schizophr. Res.* **2005,** 80, 315-322.
12. Pittaluga, A.; Vaccari, D.; Raiteri, M. The "Kynurenate Test," a Biochemical Assay for Putative Cognition Enhancers. *J. Pharmacol. Exp. Ther.* **1997,** 283, 82-90.
13. Johnson, W. S.; Woroch, E. L.; Buell, B. G. Cyclization Studies in the Quinoline Series. A New Synthesis of 4-Aminoquinolines. *J. Am. Chem. Soc.* **1949,** 71, 1901-1905.
14. Sacquet, M. C.; Maitte, P. Addition de derives maloniques sure des beta-enaminones cycliques. *J. Heterocycl. Chem.* **1985,** 22, 713-718.

15. Collins, R. F. Some Derivatives of 1,2-Dihydro- and 1,2,3,4-Tetrahydroquinoline. *J. Chem. Soc.* **1960**, 2053-2059.
16. Pellicciari, R.; Natalini, B.; Costantino, G.; Mahmoud, M. R.; Mattoli, L.; Sadeghpour, B. M.; Moroni, F.; Chiarugi, A.; Carpenedo, R. Modulation of the kynurenine pathway in search for new neuroprotective agents. Synthesis and preliminary evaluation of (m-nitrobenzoyl)alanine, a potent inhibitor of kynurenine-3-hydroxylase. *J. Med. Chem.* **1994,** 37, 647-655.
17. Varasi, M.; la Torre, A.; Heidempergher, F.; Pevarello, P.; Speciale, C.; Guidetti, P.; Wells, D. R.; Schwarcz, R. Derivatives of kynurenine as inhibitors of rat brain kynurenine aminotransferase. *Eur. J. Med. Chem.* **1996,** 31, 11-21.
18. Pellicciari, R.; Rizzo, R. C.; Costantino, G.; Marinozzi, M.; Amori, L.; Guidetti, P.; Wu, H. Q.; Schwarcz, R. Modulators of the kynurenine pathway of tryptophan metabolism: synthesis and preliminary biological evaluation of (S)-4-(ethylsulfonyl)benzoylalanine, a potent and selective kynurenine aminotransferase II (KAT II) inhibitor. *ChemMedChem* **2006,** 1, 528-531.
19. Fitzgerald, D. H.; Muirhead, K. M.; Botting, N. P. A comparative study on the inhibition of human and bacterial kynureninase by novel bicyclic kynurenine analogues. *Bioorg. Med. Chem.* **2001,** 9, 983-989.
20. Atwal, M. S.; Bauer, L.; Dixit, S. N.; Gearien, J. E.; Morris, R. W. Analgesics. Some Substituted 2,3-Dihydro-4-quinolones. *J. Med. Chem.* **1965,** 8, 566-571.
21. Schultz, E. M.; Arnold, R. T. Synthetic Studies in the Isoquinoline Series. *J. Am. Chem. Soc.* **1949,** 71, 1911-1914.
22. Pal, K. An Improved Synthesis of 5-Ethenyl-4a-methyl-2-oxo-2,3,4,4a,7,8-hexahydronaphthalene and Similar 1,3-Dienes using Palladium Catalyzed Cross-Coupling Methodology. In *Synthesis*, 1995; pp 1485-1487.
23. Nishiwaki, N.; Rahbek, K. K.; Gothelf, K. V.; Jorgensen, K. A. Catalytic Enantioselective Addition of Nitro Compounds to Imines-A Simple Approach for the Synthesis of Optically Active beta-Nitro-alpha-Amino Esters. *Angew. Chem. Int. Ed. Engl.* **2001,** 40, 2992-2995.
24. Giuseppone, N.; Van de Weghe, P.; Mellah, M.; Collin, J. Mukaiyama aldol and Michael reactions catalyzed by lanthanide iodides. *Tetrahedron* **1998,** 54, 13129-13148.
25. Porter, J. R.; Traverse, J. F.; Hoveyda, A. H.; Snapper, M. L. Three-component catalytic asymmetric synthesis of aliphatic amines. *J. Am. Chem. Soc.* **2001,** 123, 10409-10410.
26. Werbel, L. M.; Kesten, S. J.; Turner, W. R. Structure-activity relationships of antimalarial indolo[3,2-c]quinolines. *Eur. J. Med. Chem.* **1993,** 28, 837-852.
27. Pellicciari, R.; Venturoni, F.; Bellocchi, D.; Carotti, A.; Marinozzi, M.; Macchiarulo, A.; Amori, L.; Schwarcz, R. Sequence Variants in Kynurenine Aminotransferase II (KAT II) Orthologs Determine Different Potencies of the Inhibitor S-ESBA. *ChemMedChem* **2008,** 3, 1199-1202.
28. Lima, S.; Kumar, S.; Gawandi, V.; Momany, C.; Phillips, R. S. Crystal Structure of the Homo sapiens Kynureninase-3-Hydroxyhippuric Acid Inhibitor Complex: Insights into the Molecular Basis Of Kynureninase Substrate Specificity. *J. Med. Chem.* **2009,** 52, 389-396.
29. Han, Q.; Robinson, H.; Li, J. Crystal structure of human kynurenine aminotransferase II. *J. Biol. Chem.* **2008,** 283, 3567-3573.
30. Jensen, R. A.; Gu, W. Evolutionary recruitment of biochemically specialized subdivisions of Family I within the protein superfamily of aminotransferases. *J. Bacteriol.* **1996,** 178, 2161-2171.
31. Christen, P.; Mehta, P. K. From cofactor to enzymes. The molecular evolution of pyridoxal-5'-phosphate-dependent enzymes. *Chem. Rec.* **2001,** 1, 436-447.
32. Soda, K.; Yoshimura, T.; Esaki, N. Stereospecificity for the hydrogen transfer of pyridoxal enzyme reactions. *Chem. Rec.* **2001,** 1, 373-384.
33. Guidetti, P.; Okuno, E.; Schwarcz, R. Characterization of rat brain kynurenine aminotransferases I and II. *J. Neurosci. Res.* **1997,** 50, 457-465.

34. Kocki, T.; Luchowski, P.; Luchowska, E.; Wielosz, M.; Turski, W. A.; Urbanska, E. M. L-cysteine sulphinate, endogenous sulphur-containing amino acid, inhibits rat brain kynurenic acid production via selective interference with kynurenine aminotransferase II. *Neurosci. Lett.* **2003,** 346, 97-100.
35. Heidempergher, F.; Pevarello, P.; Pillan, A.; Pinciroli, V.; Della, T. A.; Speciale, C.; Marconi, M.; Cini, M.; Toma, S.; Greco, F.; Varasi, M. Pyrrolo[3,2-c]quinoline derivatives: a new class of kynurenine-3-hydroxylase inhibitors. *Farmaco* **1999,** 54, 152-160.
36. Bender, D. A.; Wynick, D. Inhibition of kynureninase (L-kynurenine hydrolase, EC 3 . 7. 1 . 3) by oestrone sulphate: an alternative explanation for abnormal results of tryptophan load tests in women receiving oestrogenic steroids. *Br. J. Nutr.* **1981,** 45, 269-275.
37. Heyes, M. P.; Quearry, B. J. Quantification of 3-hydroxykynurenine in brain by high-performance liquid chromatography and electrochemical detection. *J. Chromat. B: Biomed. Sci. Appl.* **1988,** 428, 340-344.
38. *Sybyl, Tripos Inc., 1699 South Hanley Rd., St. Louis, Missouri, 63144, USA*, 2004.
39. Sanner, M. F. Python: A Programming Language for Software Intergration and Development. *J. Mol. Graph. Model.* **1999,** 17, 57-61.
40. Trott, O.; Olson, A. J. AutoDock Vina: Improving the speed and accuracy of docking with a new scoring function, efficient optimization, and multithreading. *J. Comput. Chem.* **2009**.